

Supporting Information

Dimolybdenum Paddlewheel as Building Block for Heteromultimetallic Structures

Nicolai D. Knöfel,^[a] Christoph Schoo,^[a] Tim P. Seifert,^[a] and Peter W. Roesky^[a]*

[a] Institute of Inorganic Chemistry; Karlsruhe Institute of Technology (KIT); Engesserstraße 15,
76131 Karlsruhe, Germany; E-mail: roesky@kit.edu;

Table of Contents

Single Crystal X-Ray Diffraction	S3
Solid state structures	S6
NMR Spectra	S14
IR Spectra (ATR)	S29
Photoluminescence Spectra	S33
Bibliography	S34

Single Crystal X-Ray Diffraction

A suitable crystal was covered in mineral oil (Aldrich) and mounted on a glass fiber. The crystal was transferred directly to the cold stream of a STOE IPDS 2 or a STOE StadiVari diffractometer. All structures were solved by using the program SHELXS/T^{1, 2} and Olex2.³ The remaining non-hydrogen atoms were located from successive difference Fourier map calculations. The refinements were carried out by using full-matrix least-squares techniques on F^2 by using the program SHELXL.^{1, 2} In each case, the locations of the largest peaks in the final difference Fourier map calculations, as well as the magnitude of the residual electron densities, were of no chemical significance.

Crystallographic data (excluding structure factors) for the structures reported in this paper have been deposited with the Cambridge Crystallographic Data Centre as a supplementary publication no. 1961131-1961136. Copies of the data can be obtained free of charge on application to CCDC, 12 Union Road, Cambridge CB21EZ, UK (fax: +(44)1223-336-033; email: deposit@ccdc.cam.ac.uk).

Refinement Details:

The crystal structure of **3** contains four molecules of THF in the asymmetric unit. Two THF could not be modeled satisfactorily and were therefore removed from the electron density map using the OLEX² solvent mask.³

The crystal structure of **4** contains four and a half molecules of THF in the asymmetric unit. One and a half THF could not be modeled satisfactorily and were therefore removed from the electron density map using the OLEX² solvent mask.³

The crystal structure of **5** contains four and a half molecules of DCM in the asymmetric unit. One and a half DCM could not be modeled satisfactorily and were therefore removed from the electron density map using the OLEX² solvent mask.³

The crystal structure of **6** contains three molecules of THF in the asymmetric unit. Two THF molecules could not be modeled satisfactorily and were therefore removed from the electron density map using the OLEX² solvent mask.³

Table S1. Crystal data and structure refinement of compounds 1-3.

Compound	1	2	3
Formula	C ₆₀ H ₅₆ Mo ₂ O ₈ P ₄	C ₉₈ H ₈₄ Au ₄ F ₂₀ Mo ₂ O _{11.5} P ₄	C ₁₂₀ Cl ₄ H ₁₆₀ Mo ₂ O ₁₅ P ₄ Rh ₄
<i>D</i>_{calc.}/g·cm⁻³	1.439	1.938	1.341
<i>μ</i>/mm⁻¹	0.612	6.224	0.842
Formula Weight	1220.80	2929.27	2711.67
Colour	clear yellow	clear yellow	clear yellow
Shape	plank	plate	needle
Size/mm³	0.26×0.11×0.02	0.32×0.22×0.10	0.35×0.23×0.17
<i>T</i>/K	100	100	210
Crystal System	monoclinic	triclinic	triclinic
Space Group	<i>P</i> 2 ₁ / <i>n</i>	<i>P</i> -1	<i>P</i> -1
<i>a</i>/Å	9.9882(4)	16.7915(4)	10.8868(5)
<i>b</i>/Å	8.1550(3)	18.7734(5)	16.6804(9)
<i>c</i>/Å	34.8663(9)	19.3826(5)	20.7303(11)
<i>α</i>/°		115.497(2)	105.130(4)
<i>β</i>/°	97.262(3)	92.100(2)	102.169(4)
<i>γ</i>/°		110.887(2)	104.645(4)
<i>V</i>/Å³	2817.21(17)	5019.9(2)	3358.0(3)
<i>Z</i>	2	2	1
<i>Z</i>'	0.5	1	0.5
Wavelength/Å	0.71073	0.71073	0.71073
Radiation type	MoK _α	MoK _α	MoK _α
<i>Q</i>_{min}/°	2.065	1.195	1.968
<i>Q</i>_{max}/°	26.048	26.134	26.172
Measured Refl.	14104	42389	23197
Independent Refl.	5444	19696	13020
Reflections Used	4492	15347	9237
<i>R</i>_{int}	0.0383	0.0469	0.0590
Parameters	334	1261	595
Restraints	0	149	106
Largest Peak	0.723	4.655	1.227
Deepest Hole	-0.423	-1.740	-1.152
Goof	0.960	1.015	1.015
<i>wR</i>₂ (all data)	0.0709	0.1579	0.1868
<i>wR</i>₂	0.0677	0.1480	0.1703
<i>R</i>₁ (all data)	0.0385	0.0709	0.0797
<i>R</i>₁	0.0294	0.0560	0.0595

Table S2. Crystal data and structure refinement of compounds 4-6.

Compound	4	5	6
Formula	C ₁₂₀ Cl ₄ H ₁₆₀ Ir ₄ Mo ₂ O ₁₅ P ₄	C ₁₀₉ Cl ₂₆ H ₁₃₀ Mo ₂ O ₈ P ₄ Ru ₄	Au ₄ C ₈₄ Cl ₄ H ₁₀₄ Mo ₂ O ₁₄ P ₄
D_{calc.}/g·cm⁻³	1.518	1.614	1.712
μ/mm⁻¹	4.311	1.255	6.299
Formula Weight	3068.83	3209.86	2583.09
Colour	clear orange	clear red	clear colourless
Shape	prism	prism	plate
Size/mm³	0.40×0.30×0.20	0.24×0.15×0.06	0.25×0.13×0.06
T/K	210	150	150
Crystal System	triclinic	triclinic	orthorhombic
Space Group	<i>P</i> -1	<i>P</i> -1	<i>Pbcn</i>
a/Å	10.8365(3)	11.4314(10)	21.6562(7)
b/Å	16.7623(5)	17.3797(13)	18.6547(7)
c/Å	20.7559(6)	17.3723(16)	24.8118(7)
α/°	105.261(2)	91.633(7)	
β/°	102.501(2)	100.343(7)	
γ/°	104.496(2)	102.881(6)	
V/Å³	3356.71(17)	3301.4(5)	10023.7(6)
Z	1	1	4
Z'	0.5	0.5	0.5
Wavelength/Å	0.71073	0.71073	0.71073
Radiation type	MoK _α	MoK _α	MoK _α
Q_{min}/°	1.967	1.635	1.658
Q_{max}/°	26.092	26.242	26.132
Measured Refl.	23004	23611	31447
Independent Refl.	13040	12919	9867
Reflections Used	10554	8089	5107
R_{int}	0.0341	0.0811	0.1089
Parameters	631	655	406
Restraints	132	0	150
Largest Peak	1.382	2.031	2.786
Deepest Hole	-0.800	-1.988	-1.529
Goof	1.039	1.033	1.004
wR₂ (all data)	0.1125	0.2812	0.2283
wR₂	0.1042	0.2387	0.1819
R₁ (all data)	0.0487	0.1407	0.1423
R₁	0.0365	0.0932	0.0737

Solid state structures

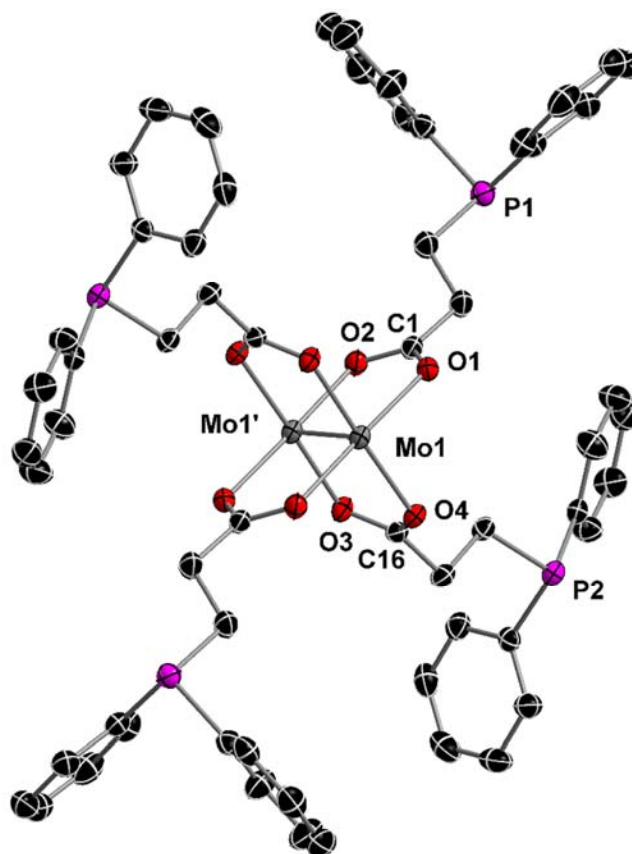


Figure S1. Molecular structure of **1** in the solid state, displayed with an ellipsoid probability of 50 %. Hydrogen atoms are omitted for clarity. Selected bond lengths [Å] and angles [°]: Mo1-Mo1' 2.1134(4), Mo1-O1 2.109(2), Mo1'-O2 2.112(2), Mo1-O3 2.110(2), Mo1-O4 2.128(2), O1-C1 1.276(3), O2-C1 1.270(3), O3-C16 1.280(3), O4-C16 1.271(3). Mo1'-Mo1-O4 90.42(4), O1-Mo1-Mo1' 92.00(4), O1-Mo1-O4 86.76(6), O2-Mo1'-Mo1 91.03(4), O3-Mo1'-Mo1 92.72(4), O3-Mo1'-O2 86.74(7), O2-C1-O1 121.8(2), O4-C16-O3 121.9(2).

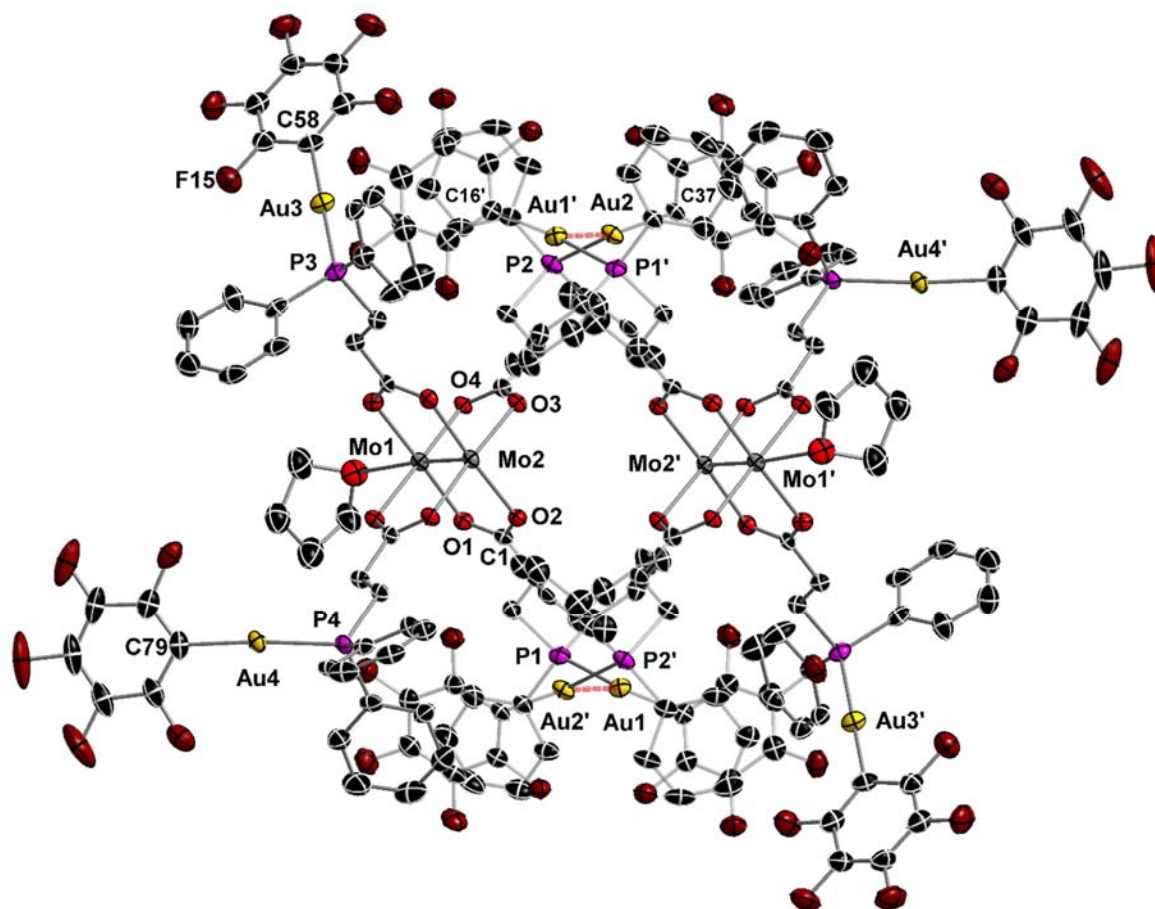


Figure S3. Molecular structure of **2** (\cdot 2 thf) in the solid state, displayed with an ellipsoid probability of 30%. Hydrogen atoms and non-coordinating solvent molecules (THF) are omitted for clarity. Selected bond lengths [\AA] and angles [$^\circ$]: Mo1-Mo2 2.0904(9), Mo1-O1 2.118(5), Mo1-O4 2.112(5), Mo2-O2 2.094(5), Mo2-O3 2.090(5), O1-C1 1.275(10), O2-C1 1.279(10), Au1-P1 2.282(2), Au2-P2 2.280(2), Au3-P3 2.273(2), Au4-P4 2.272(2). Mo2-Mo1-O1 91.4(2), Mo1-Mo2-O2 92.5(2), Mo2-Mo1-O4 91.2(2), O3-Mo2-Mo1 92.6(2), O4-Mo1-O1 90.5(2), O3-Mo2-O2 90.8(2), P1-Au1-Au2' 105.31(5), P2-Au2-Au1' 105.07(5), C16-Au1-P1 169.8(2), C37-Au2-P2 169.8(2), C58-Au3-P3 177.8(3), C79-Au4-P4 175.8(3), O1-C1-O2 122.1(7). Gold-gold distance [\AA]: Au1-Au2' 3.2198(4).

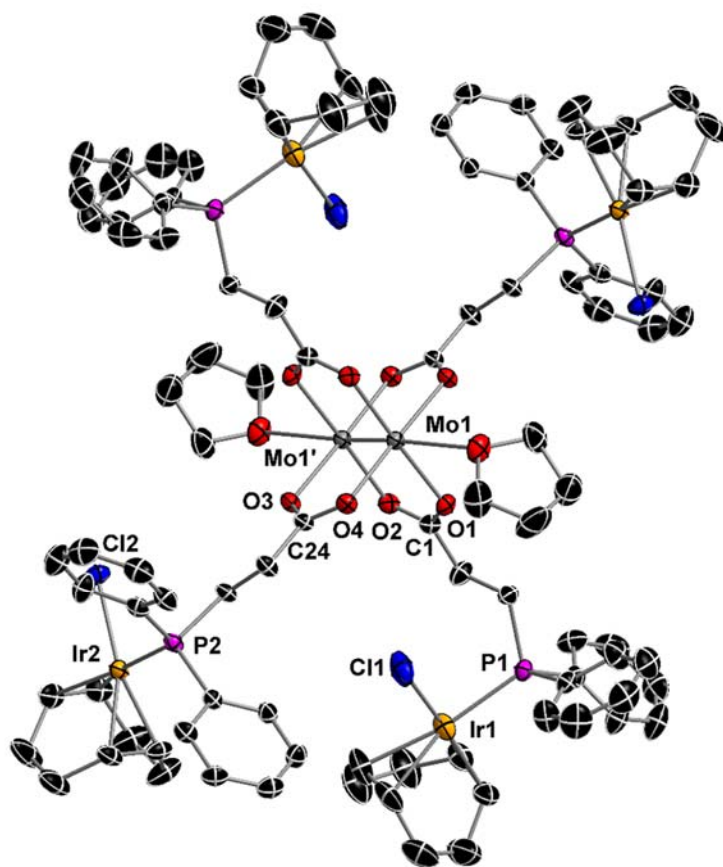


Figure S5. Molecular structure of **4** (\cdot 2 thf) in the solid state, displayed with an ellipsoid probability of 30%. Hydrogen atoms and non-coordinating solvent molecules (THF) are omitted for clarity. Selected bond lengths [\AA] and angles [$^\circ$]: Mo1-Mo1' 2.1005(8), Mo1-O1 2.126(3), Mo1'-O2 2.115(3), Mo1'-O3 2.108(3), Mo1-O4 2.117(3), Ir1-P1 2.3041(14), Ir2-P2 2.3127(13), Ir1-Cl1 2.360(2), Ir2-Cl2 2.3575(13), O1-C1 1.276(6), O2-C1 1.266(6), O3-C24 1.280(6), O4-C24 1.268(6). Mo1'-Mo1-O1 90.72(9), Mo1-Mo1'-O2 92.85(9), Mo1-Mo1'-O3 91.14(9), Mo1'-Mo1-O4 92.34(9), O4-Mo1-O1 89.07(13), O4-Mo1-O1 89.07(13), P1-Ir1-Cl1 89.23(6), P2-Ir2-Cl2 89.77(5), O2-C1-O1 122.9(4), O4-C24-O3 122.0(4).

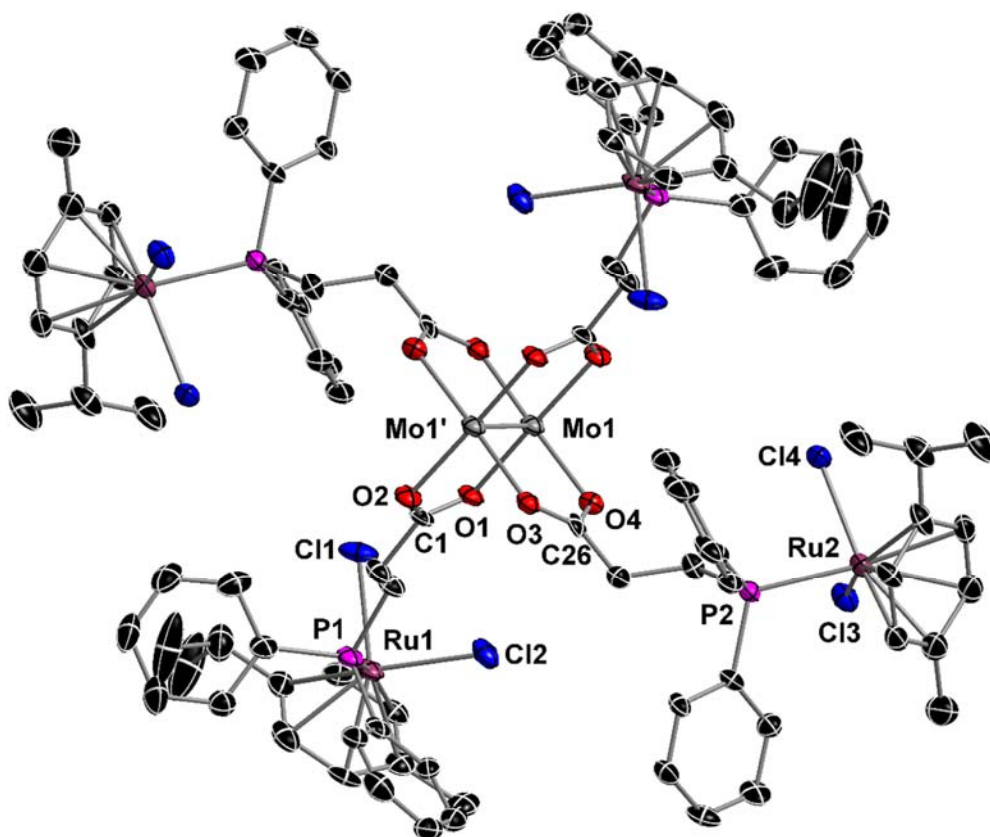


Figure S6. Molecular structure of **5** in the solid state, displayed with an ellipsoid probability of 30 %. Hydrogen atoms and solvent molecules (DCM) are omitted for clarity. Selected bond lengths [Å] and angles [°]: Mo1-Mo1' 2.079(2), Mo1-O1 2.115(6), Mo1'-O2 2.112(6), Mo1'-O3 2.088(7), Mo1-O4 2.103(7), Ru1-P1 2.347(3), Ru2-P2 2.338(2), Ru1-Cl1 2.402(3), Ru1-Cl2 2.421(3), Ru2-Cl3 2.423(3), Ru2-Cl4 2.421(3), O1-C1 1.258(12), O2-C1 1.269(13). Mo1'-Mo1-O1 91.8(2), Mo1-Mo1'-O2 91.9(2), Mo1-Mo1'-O3 92.4(2), Mo1'-Mo1-O4 91.2(2), O3-Mo1'-O2 89.9(3), O4-Mo1-O1 89.8(3), P1-Ru1-Cl1 86.84(11), P1-Ru1-Cl2 85.08(10), P2-Ru2-Cl3 87.44(9), P2-Ru2-Cl4 84.75(9), Cl1-Ru1-Cl2 88.68(12), Cl4-Ru2-Cl3 88.00(11), O1-C1-O2 122.6(8), O4-C26-O3 121.6(9).

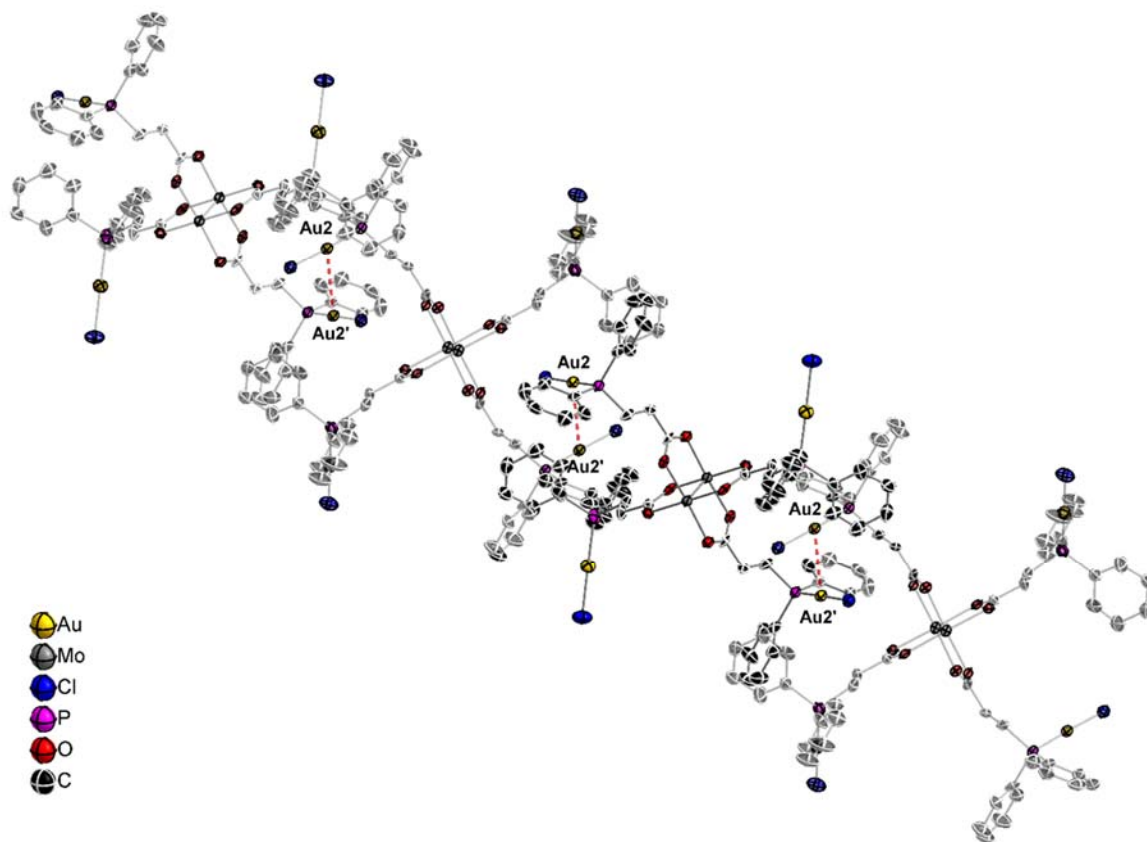


Figure S8. Excerpt of the extended solid-state structure of compound **6** ($\cdot 2$ thf), displayed with an ellipsoid probability of 30 %. Hydrogen atoms and non-coordinating solvent molecules (THF) are omitted for clarity. Formation of a 1D coordination polymer structure in the solid state due to intermolecular aurophilic interactions between Au2-Au2'. Gold-gold distance Au2-Au2' (red, dotted): 3.1427(12) Å.

NMR Spectra

NMR spectra were recorded on a Bruker Ascend 400 MHz spectrometer. ^1H and $^{13}\text{C}\{^1\text{H}\}$ NMR chemical shifts were referenced to the residual ^1H and ^{13}C resonances of the deuterated solvents and are reported relative to tetramethylsilane. $^{31}\text{P}\{^1\text{H}\}$ and $^{19}\text{F}\{^1\text{H}\}$ NMR resonances were referenced to external 85 % phosphoric acid and CFCl_3 , respectively.

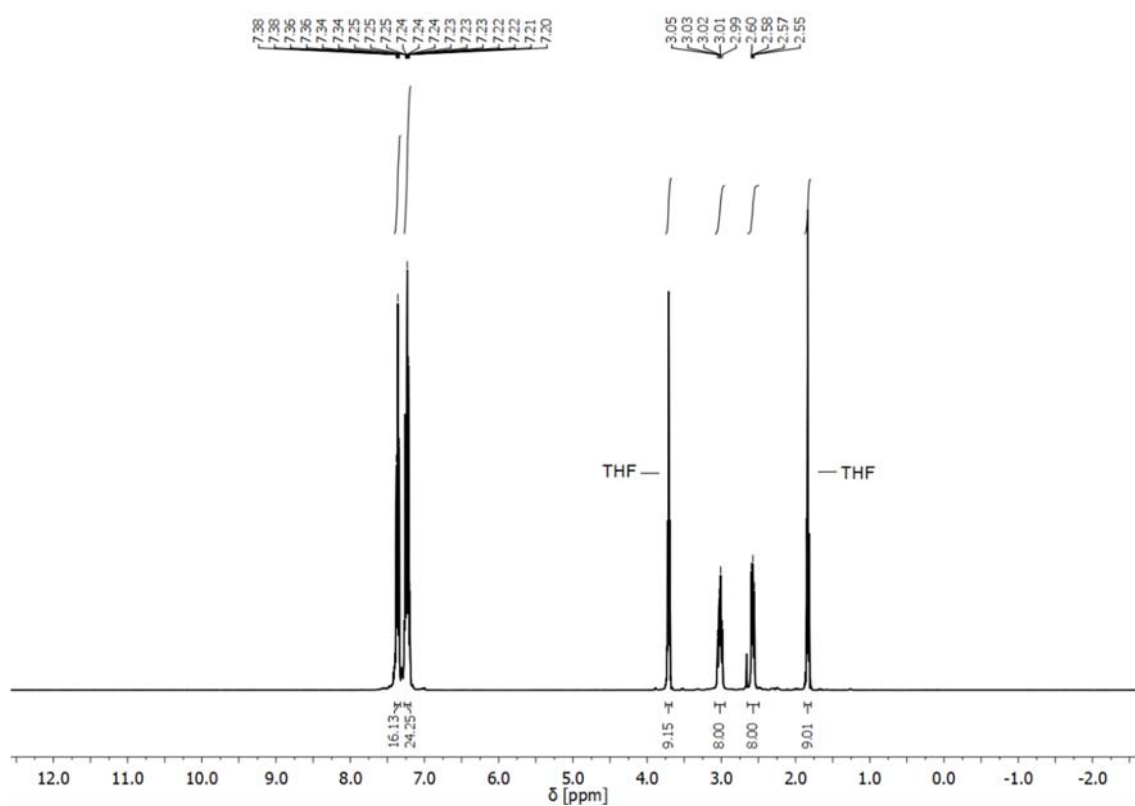


Figure S9. ^1H NMR spectrum of compound **1** in CDCl_3 (400 MHz; 298 K).

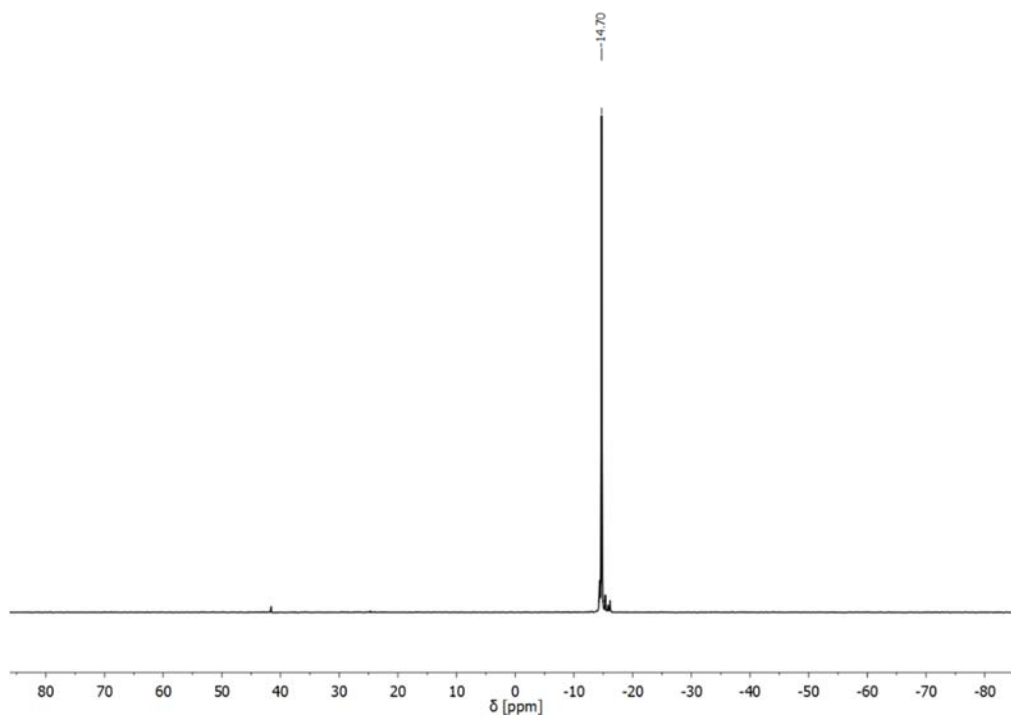


Figure S10. $^{31}\text{P}\{^1\text{H}\}$ NMR spectrum of compound **1** in CDCl_3 (162 MHz; 298 K).

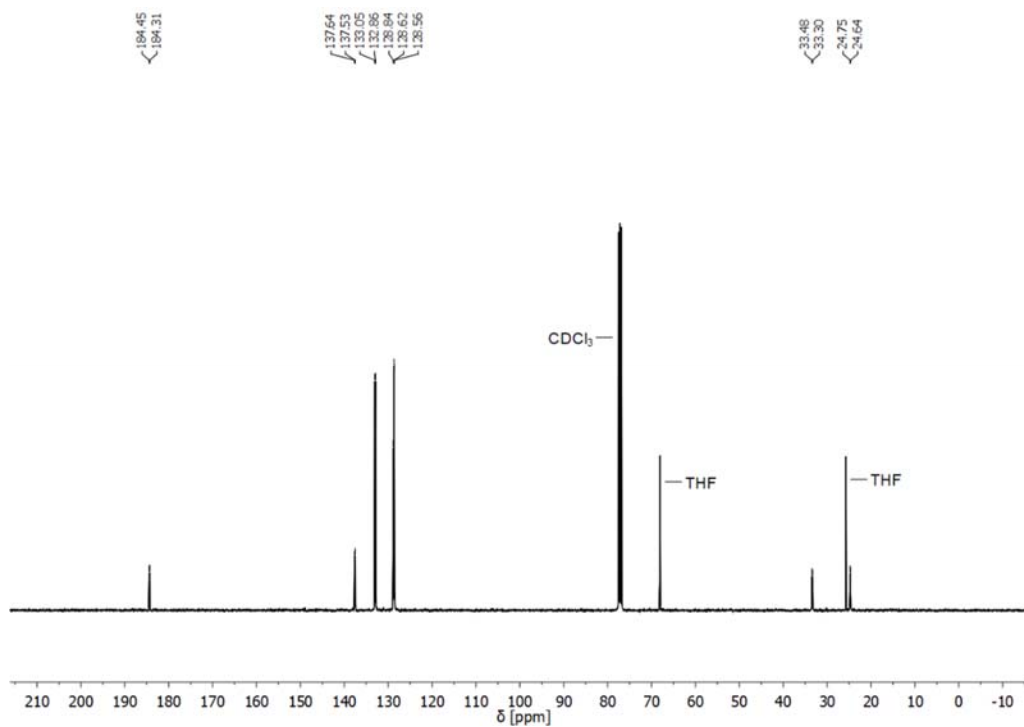


Figure S11. $^{13}\text{C}\{^1\text{H}\}$ NMR spectrum of compound **1** in CDCl_3 (101 MHz; 298 K).

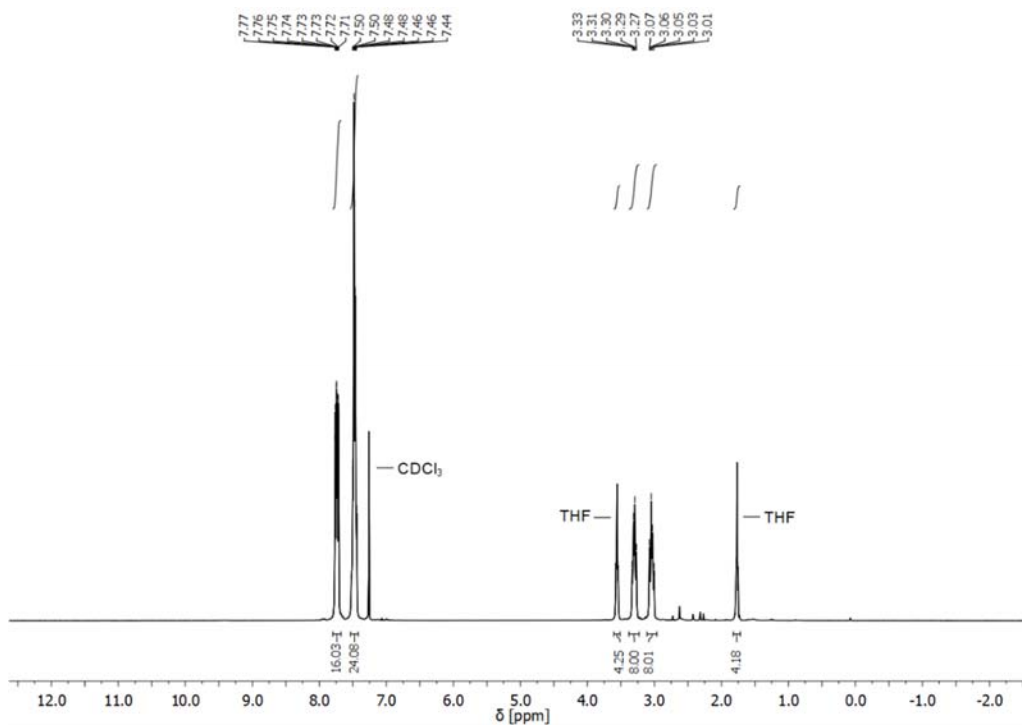


Figure S12. ^1H NMR spectrum of compound **2** in CDCl_3 (400 MHz; 298 K).

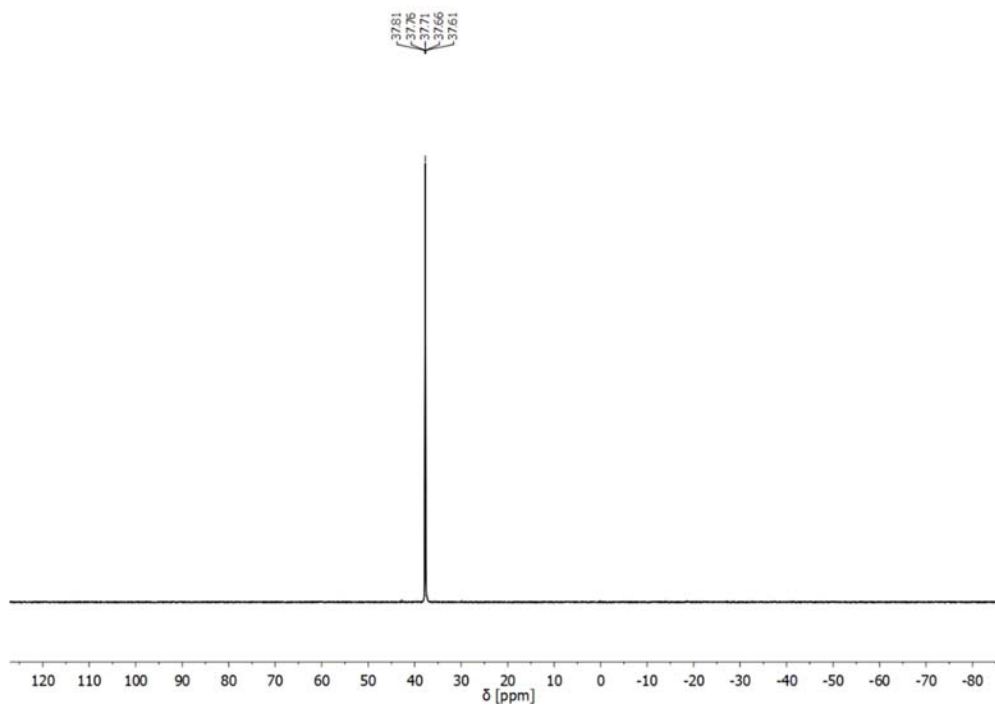


Figure S13. $^{31}\text{P}\{^1\text{H}\}$ NMR spectrum of compound **2** in CDCl_3 (162 MHz; 298 K).

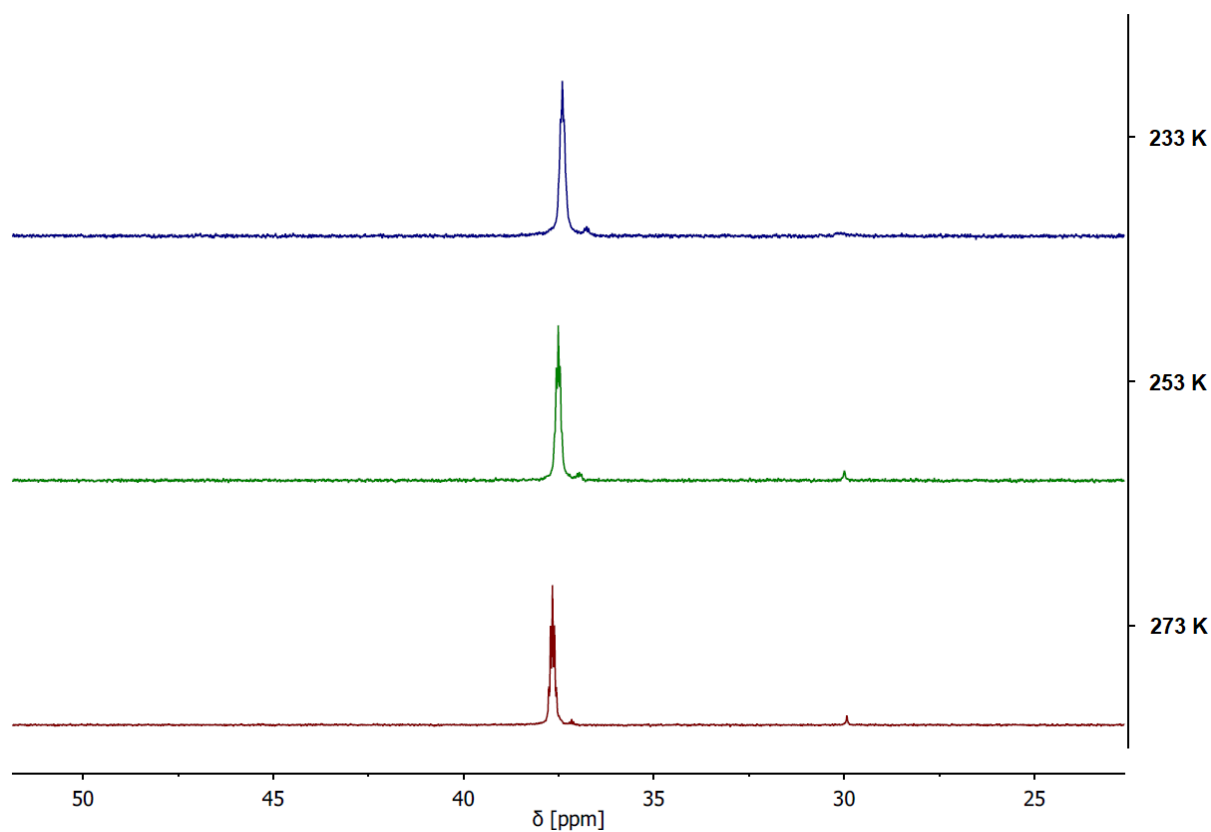


Figure S14. $^{31}\text{P}\{^1\text{H}\}$ NMR spectra of compound **2** in CDCl_3 (162 MHz) at different temperatures (273 K – 233 K). In every spectrum a single resonance for the AuC_6F_5 coordinated phosphine moieties is detected (resonance splitting of a pseudo-quintet, refer to Fig. S15). A decrease in temperature merely results in a slightly broadened resonance and a slight upfield chemical shift ($\delta = 37.7$ ppm at 273 K to $\delta = 37.4$ ppm at 233 K), which is merely a temperature induced effect. This indicates no direct gold(I) interactions in solution (or a symmetric behavior of the dimeric structure), in contrast to the solid state (Figure S3).

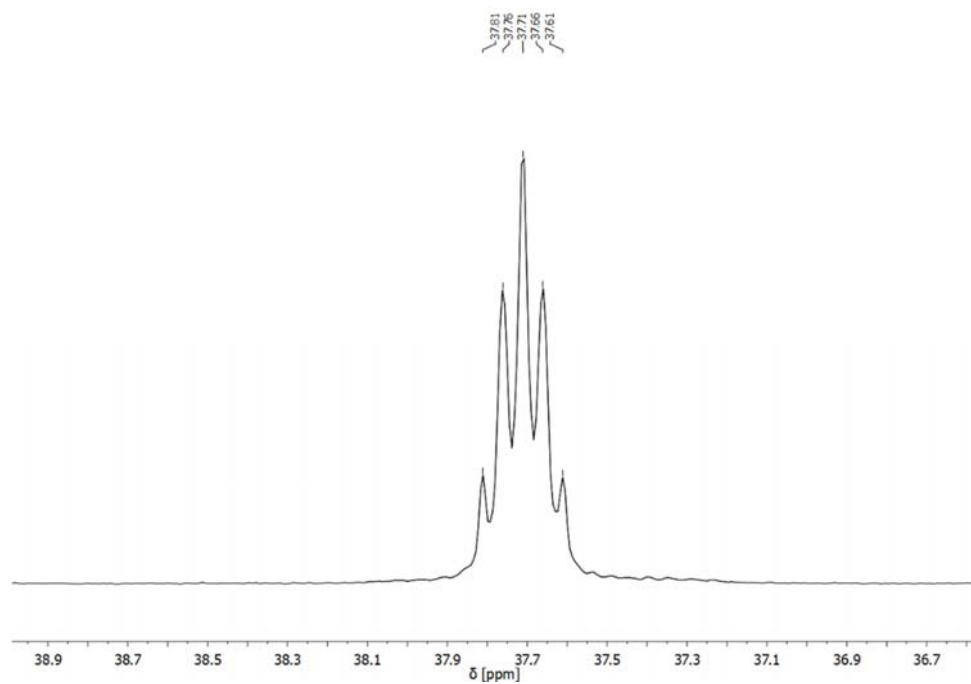


Figure S14. $^{31}\text{P}\{^1\text{H}\}$ NMR spectrum of compound **2** in CDCl₃ (162 MHz; 298 K); Resonance splitting of a pseudo-quintet, due to a long-range phosphor coupling to the fluorine atoms of the C₆F₅ ligands.

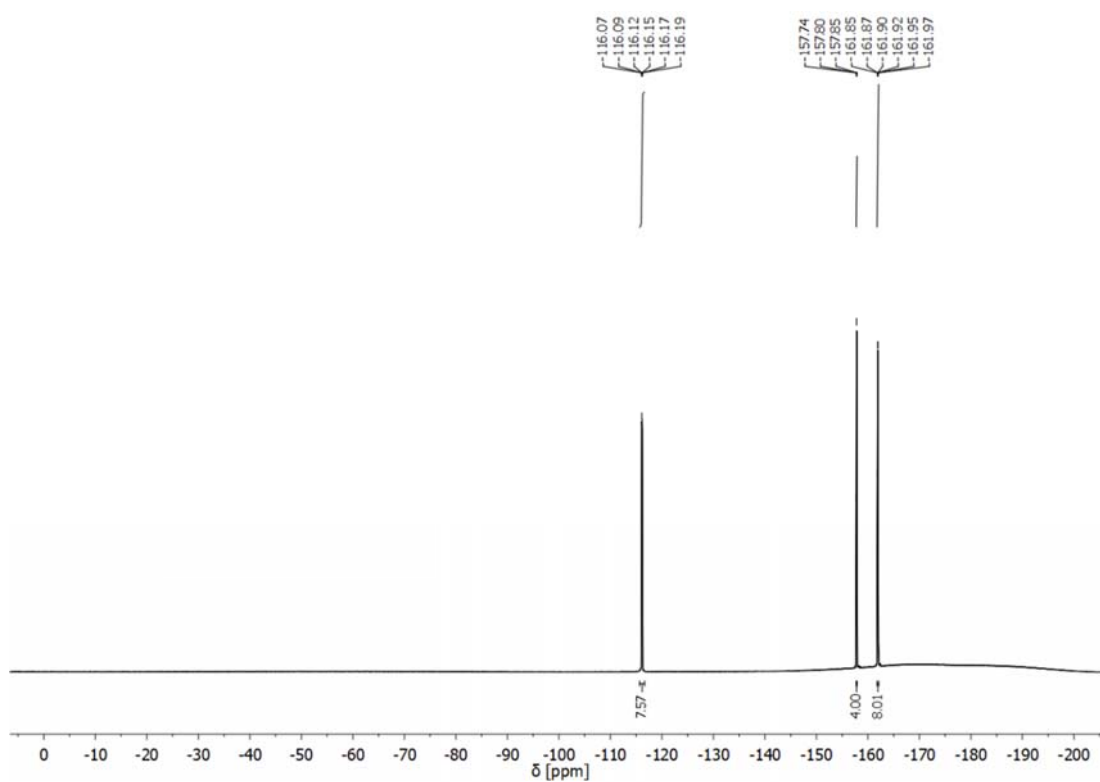


Figure S15. $^{19}\text{F}\{^1\text{H}\}$ NMR spectrum of compound **2** in CDCl₃ (377 MHz; 298 K).

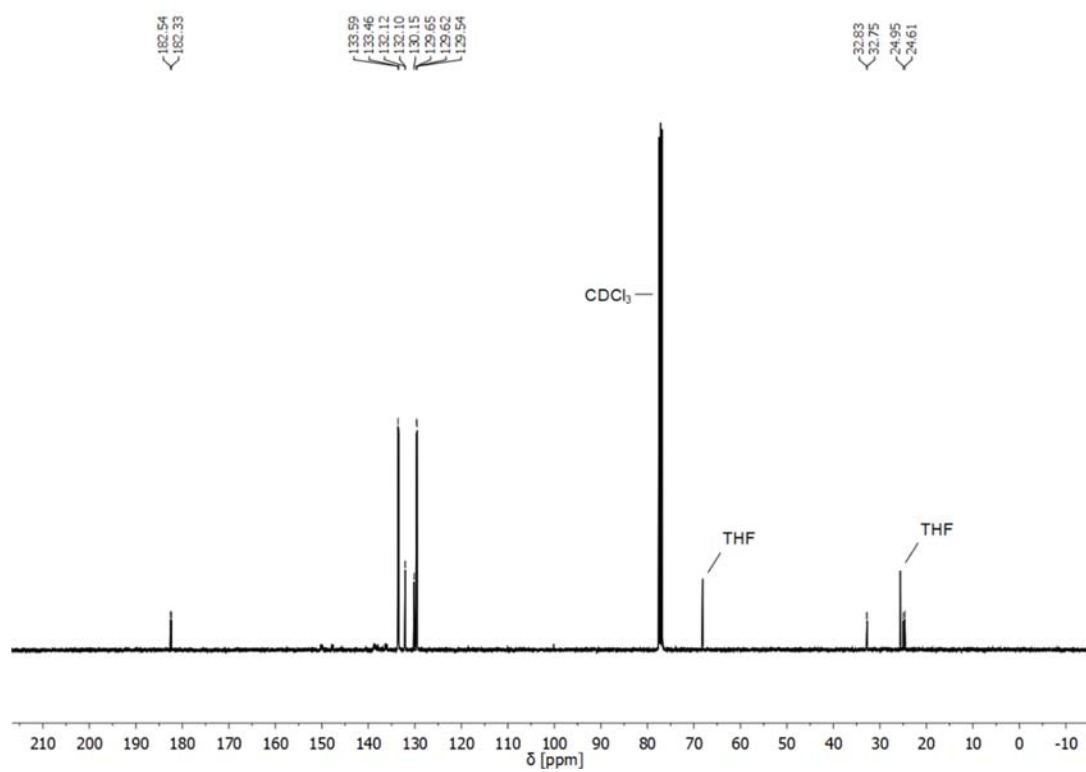


Figure S16. $^{13}\text{C}\{^1\text{H}\}$ NMR spectrum of compound **2** in CDCl_3 (101 MHz; 298 K).

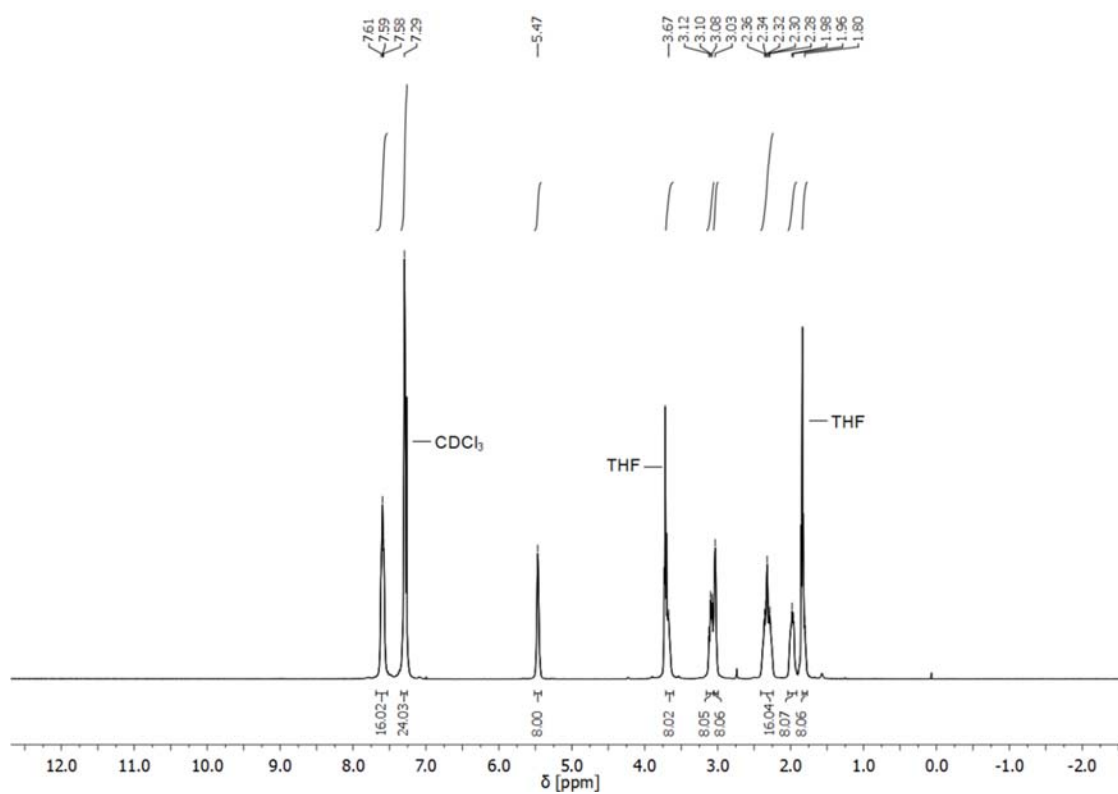


Figure S17. ^1H NMR spectrum of compound **3** in CDCl_3 (400 MHz; 298 K).

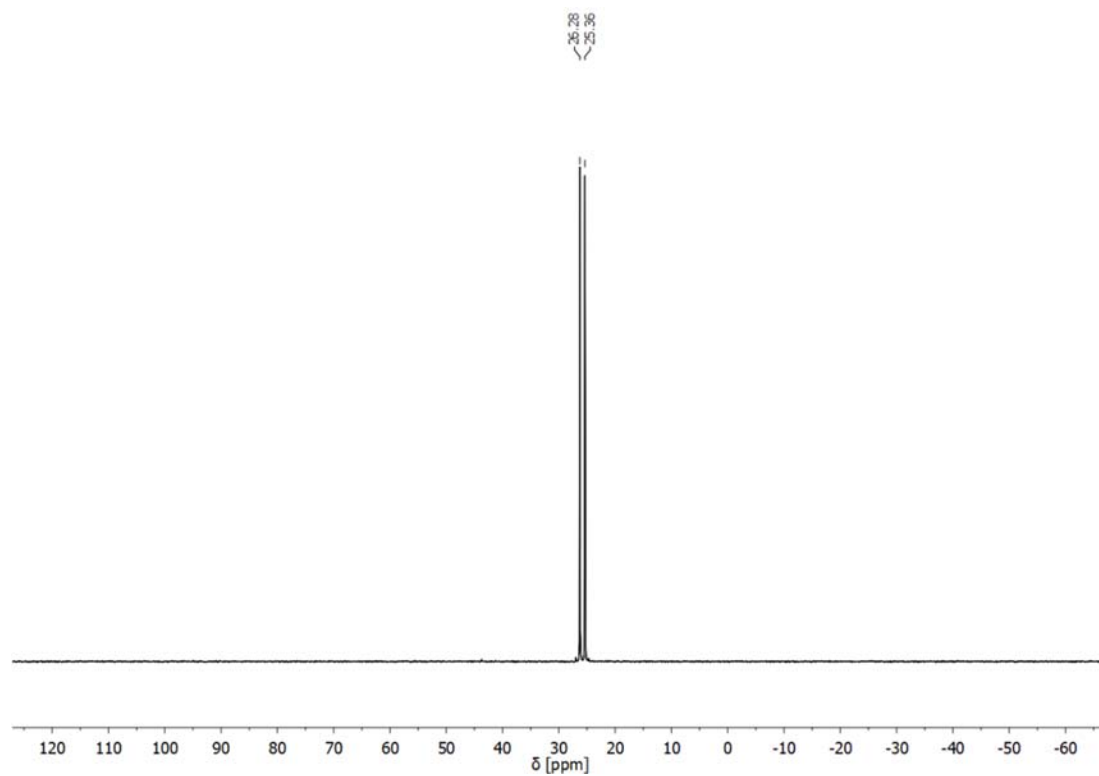


Figure S18. $^{31}\text{P}\{^1\text{H}\}$ NMR spectrum of compound **3** in CDCl_3 (162 MHz; 298 K).

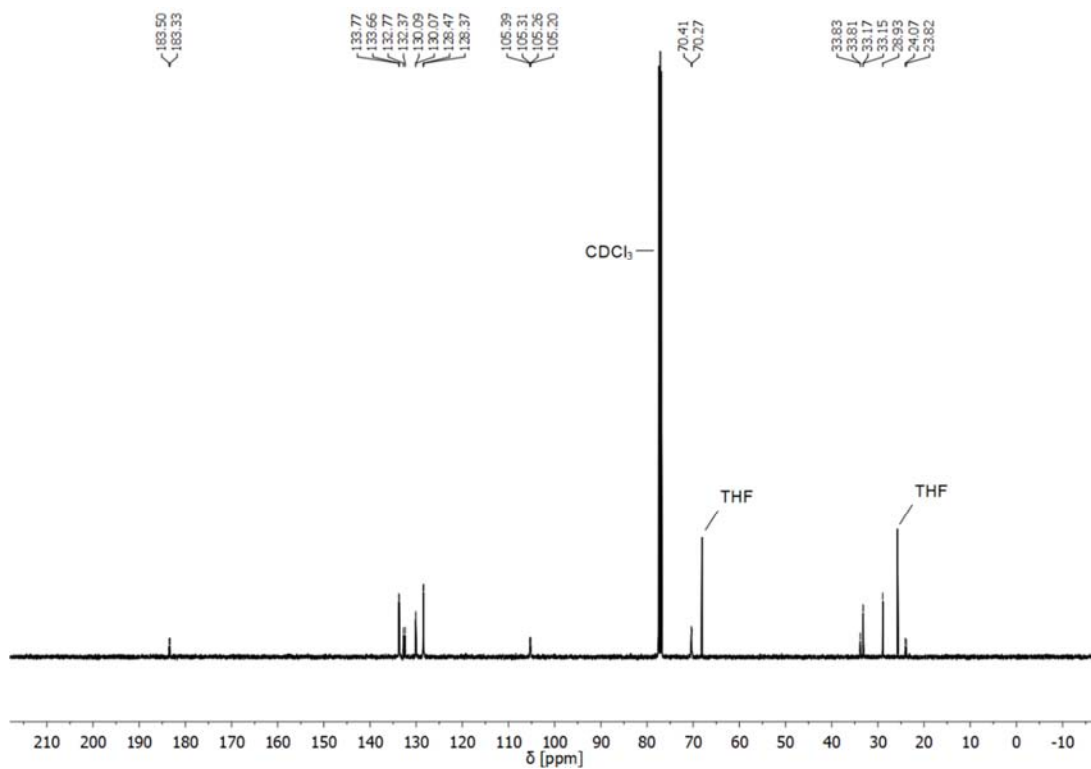


Figure S20. $^{13}\text{C}\{^1\text{H}\}$ NMR spectrum of compound **3** in CDCl_3 (101 MHz; 298 K).

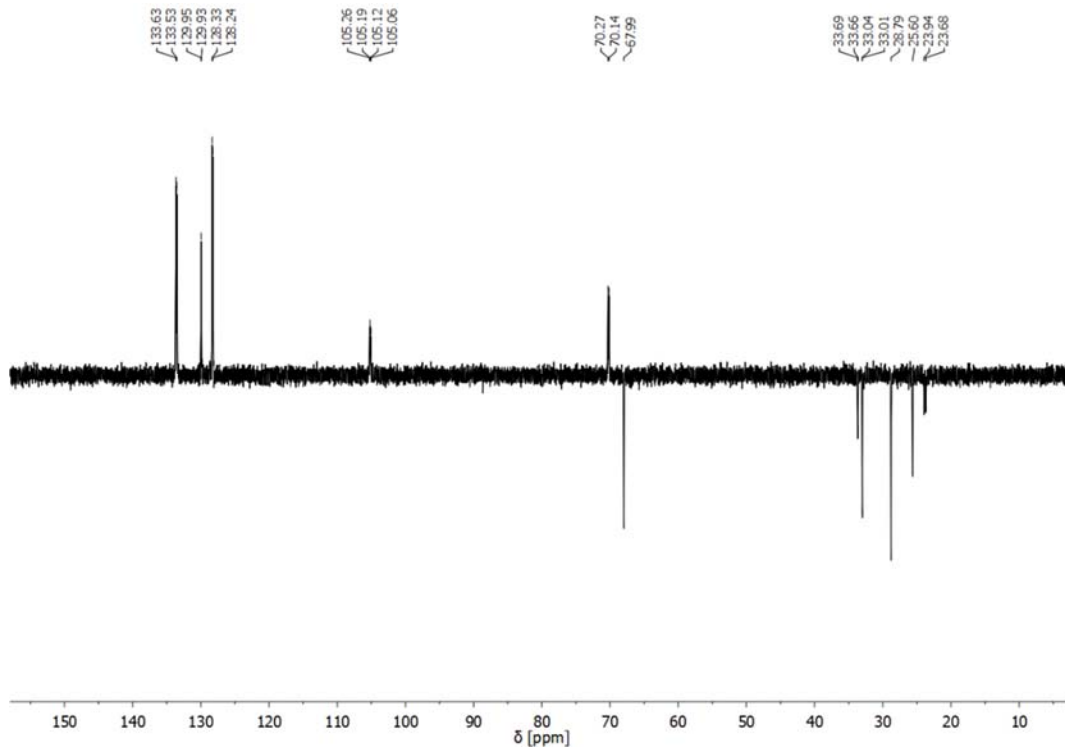


Figure S19. DEPT spectrum of compound **3** in CDCl_3 (101 MHz; 298 K).

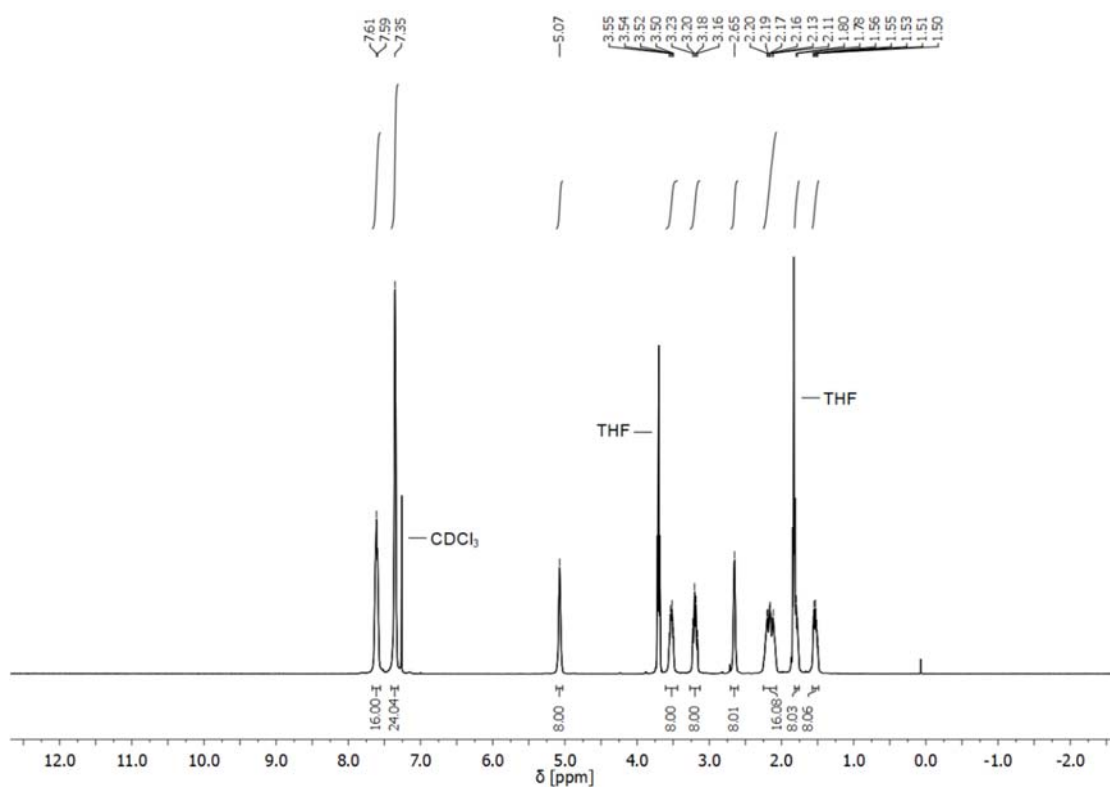


Figure S20. ¹H NMR spectrum of compound **4** in CDCl₃ (400 MHz; 298 K).

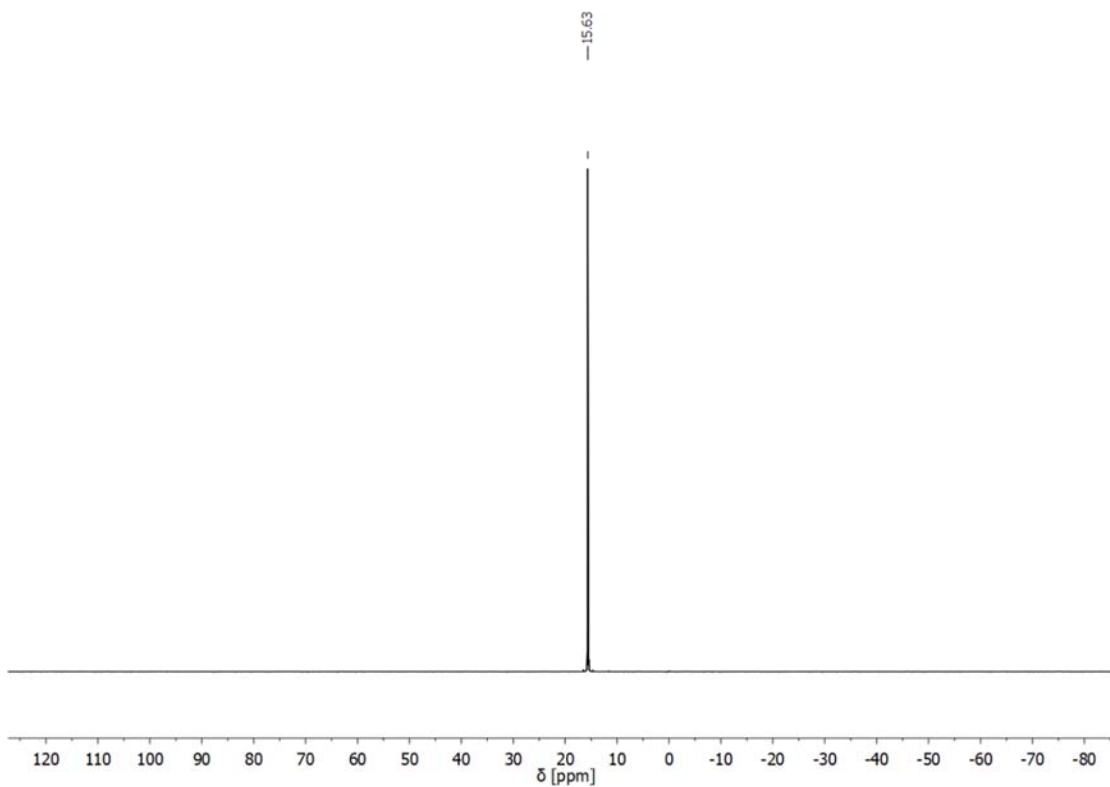


Figure S21. ³¹P{¹H} NMR spectrum of compound **4** in CDCl₃ (162 MHz; 298 K).

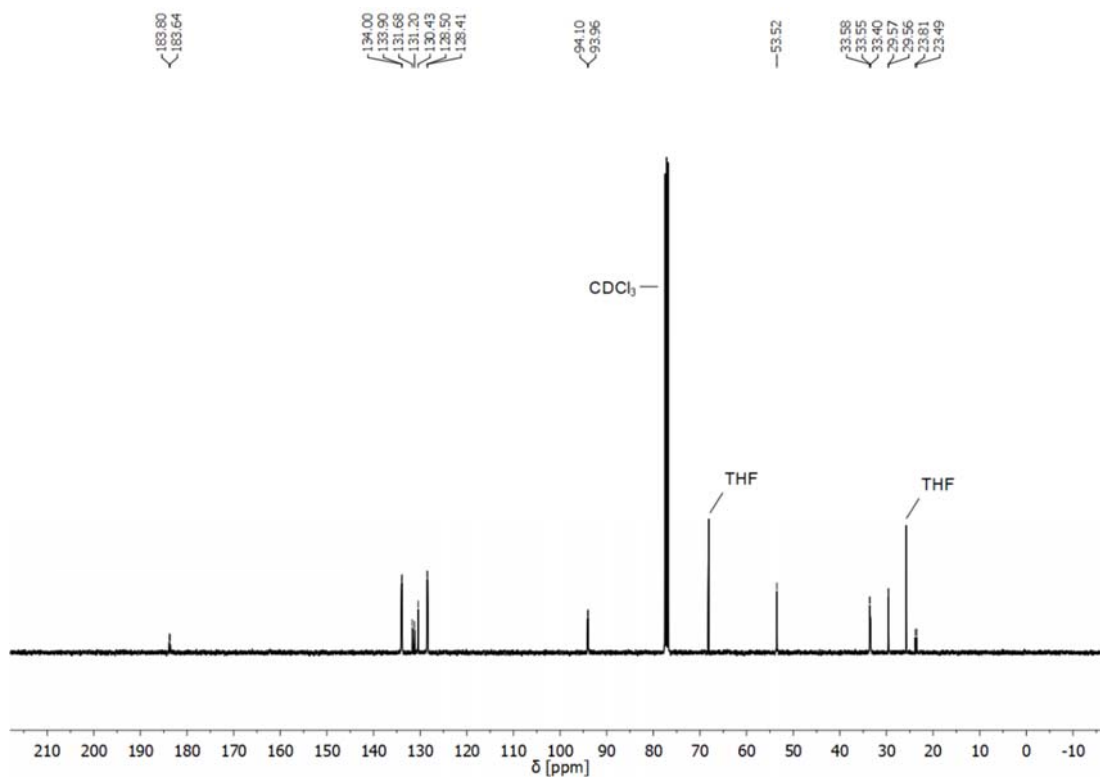


Figure S22. $^{13}\text{C}\{^1\text{H}\}$ NMR spectrum of compound **4** in CDCl_3 (101 MHz; 298 K).

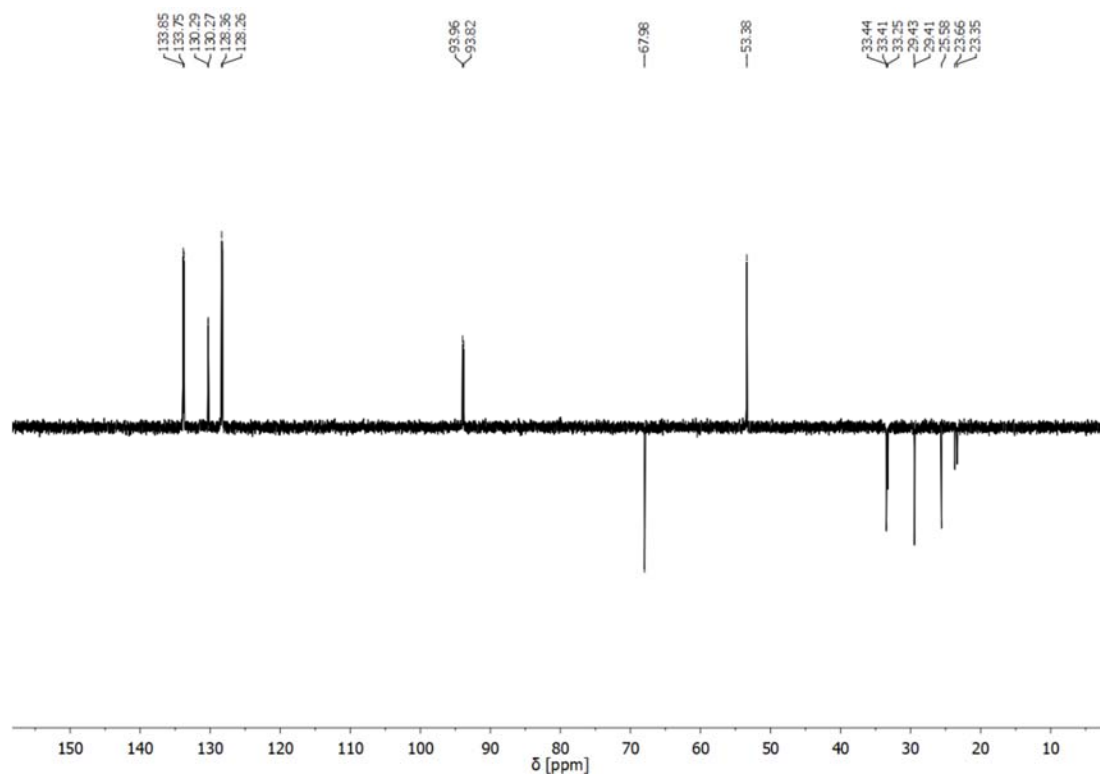


Figure S23. DEPT spectrum of compound **4** in CDCl_3 (101 MHz; 298 K).

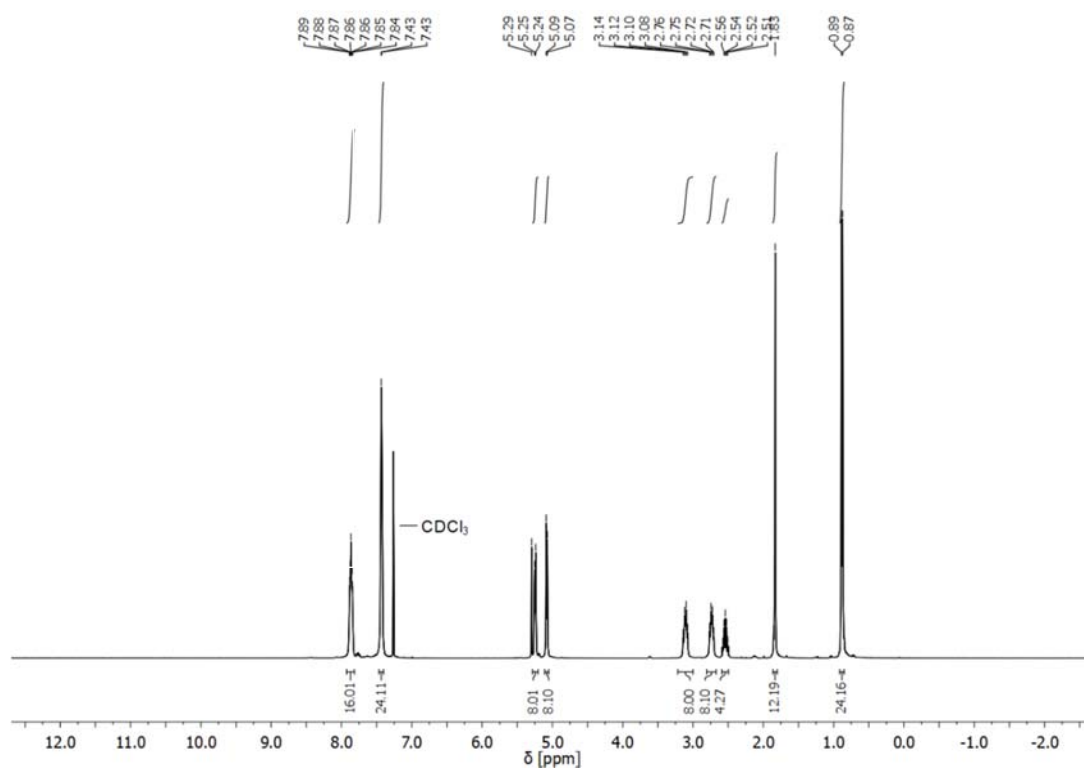


Figure S24. ^1H NMR spectrum of compound **5** in CDCl_3 (400 MHz; 298 K).

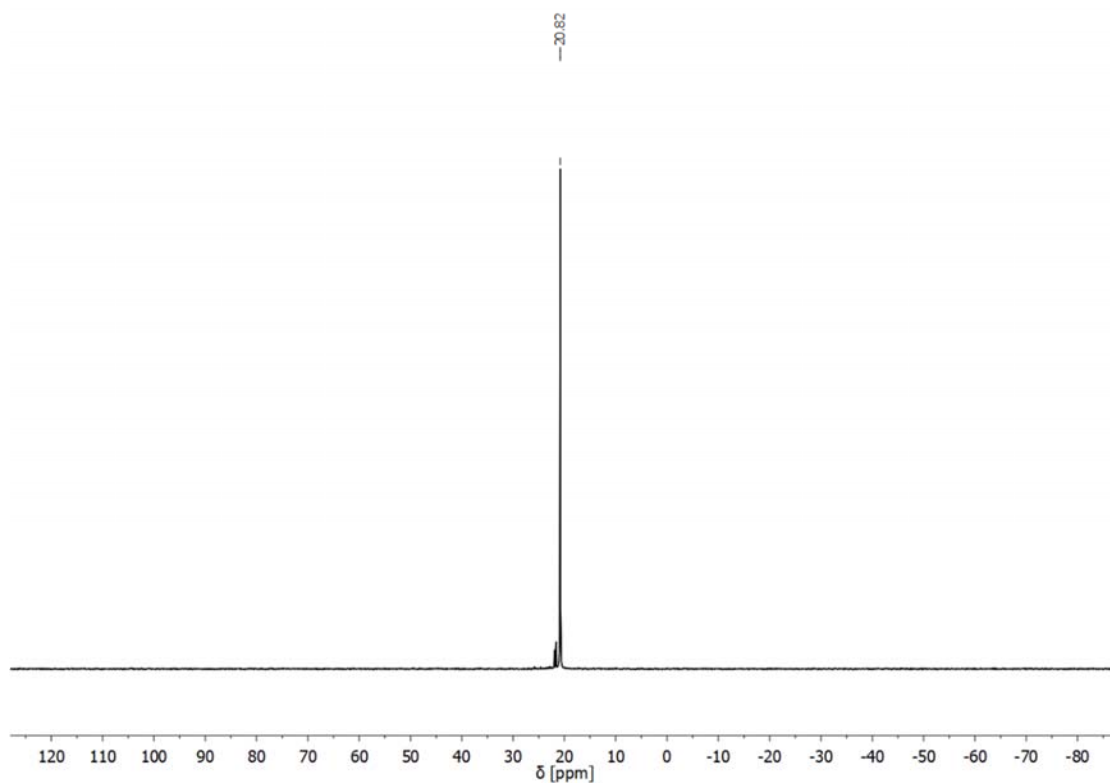


Figure S25. $^{31}\text{P}\{^1\text{H}\}$ NMR spectrum of compound **5** in CDCl_3 (162 MHz; 298 K).

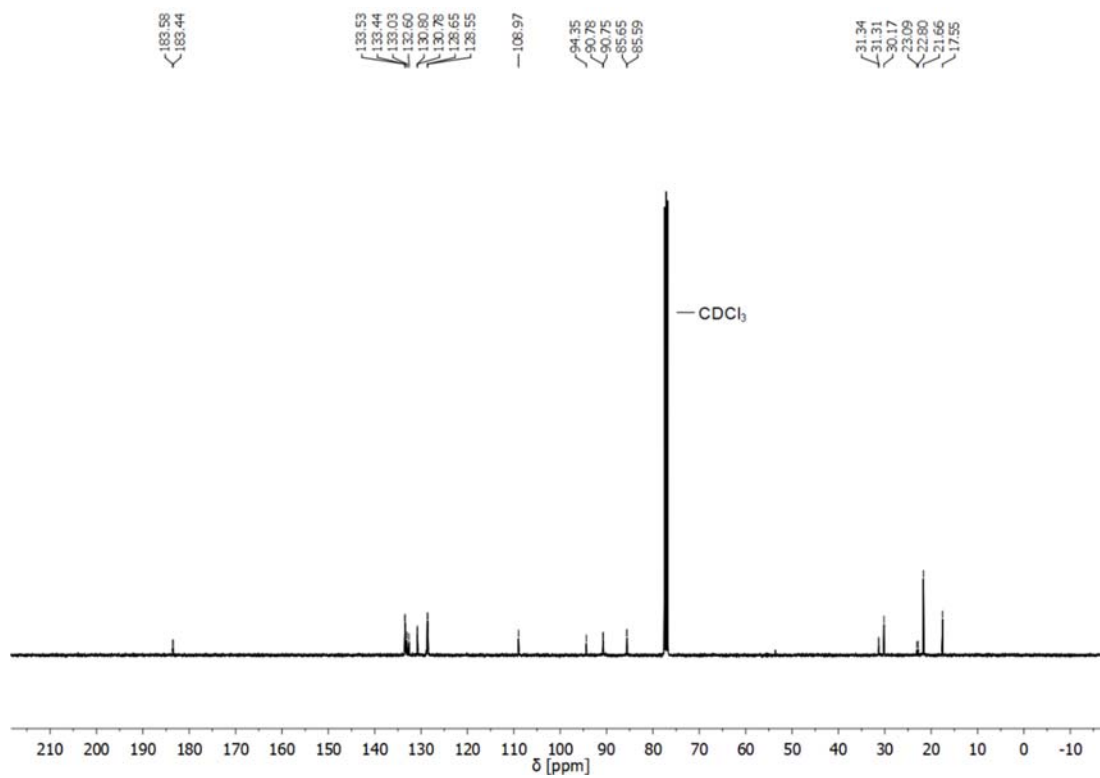


Figure S26. $^{13}\text{C}\{^1\text{H}\}$ NMR spectrum of compound **5** in CDCl_3 (101 MHz; 298 K).

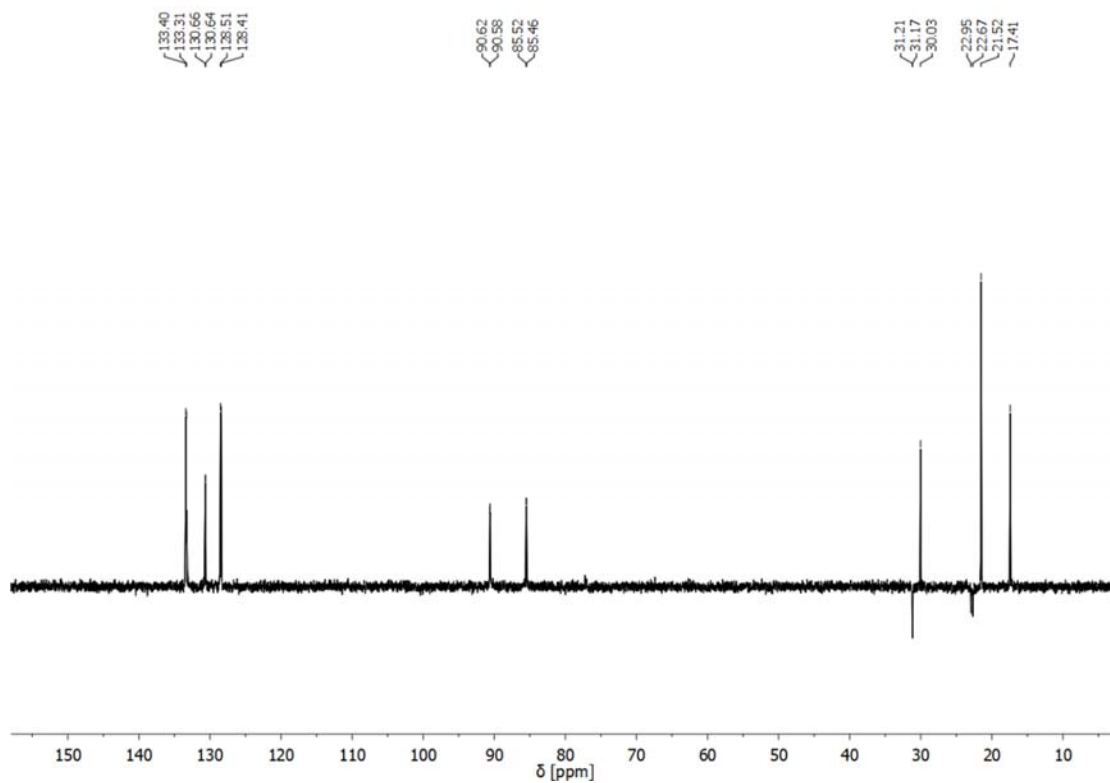


Figure S27. DEPT spectrum of compound **5** in CDCl_3 (101 MHz; 298 K).

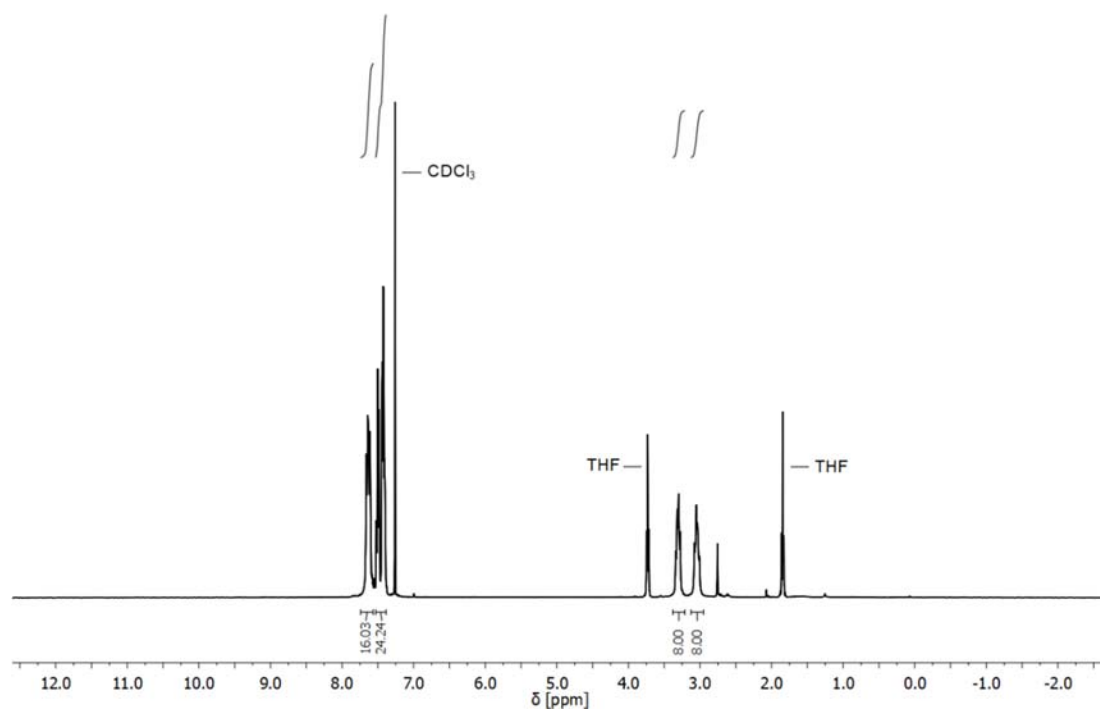


Figure S30. ^1H NMR spectrum of compound **6** in CDCl_3 (400 MHz; 298 K).

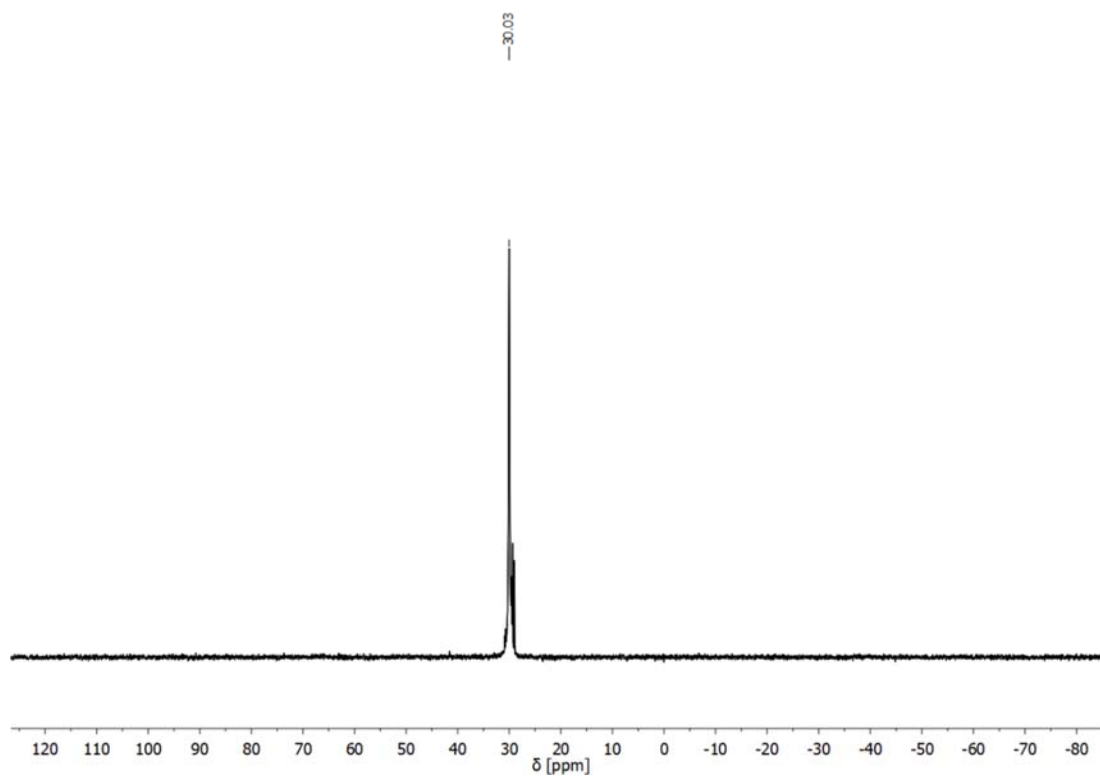


Figure S28. $^{31}\text{P}\{^1\text{H}\}$ NMR spectrum of compound **6** in CDCl_3 (162 MHz; 298 K).

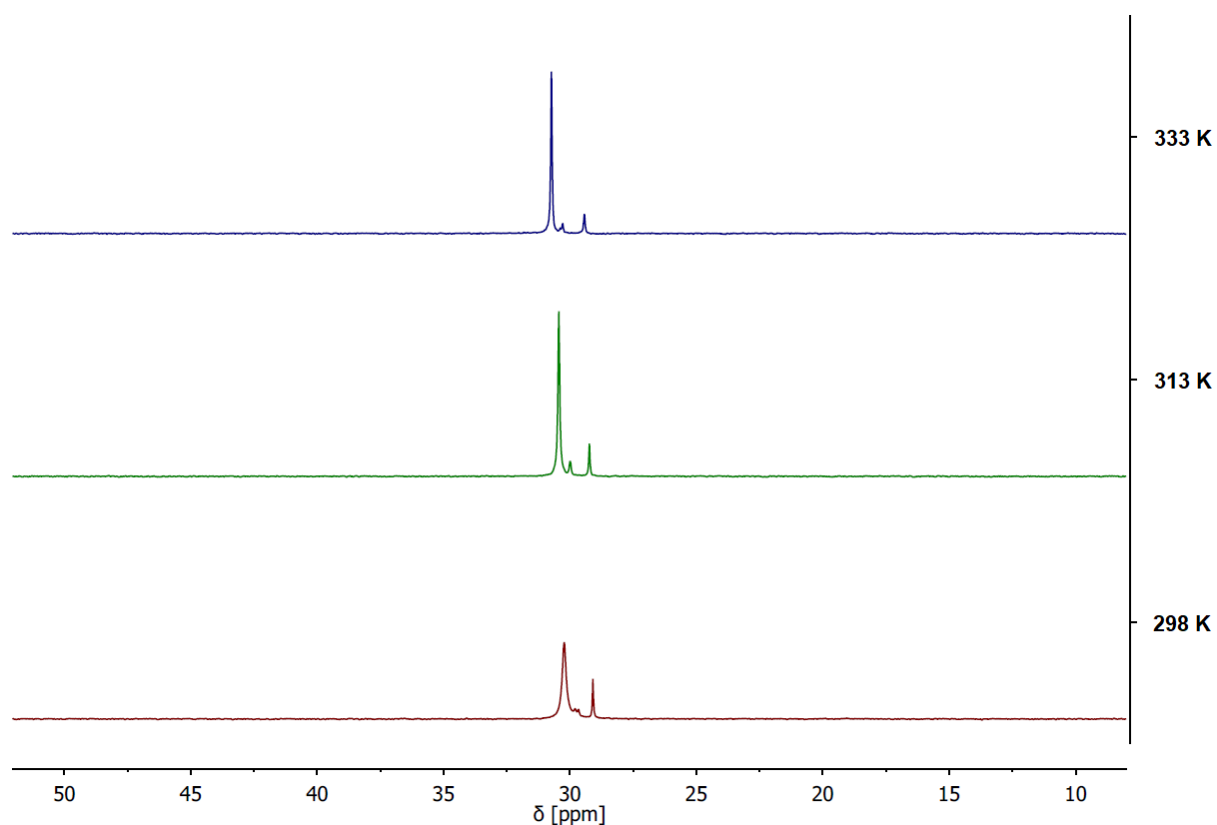


Figure S29. $^{31}\text{P}\{^1\text{H}\}$ NMR spectra of compound **6** in CDCl_3 (162 MHz) at different temperatures (298 K – 333 K). In every spectrum a set of resonances for the AuCl coordinated phosphine moieties is detected (refer to Fig. S31), indicating slightly different chemical environments. An increase in temperature merely results in a sharpening of the main resonance and a slight downfield chemical shift ($\delta = 30.2$ ppm at 298 K to $\delta = 30.7$ ppm at 333 K), which is a temperature induced effect. This may indicate aurophilic interactions in solution, as varying resonances are observed even at elevated temperatures.

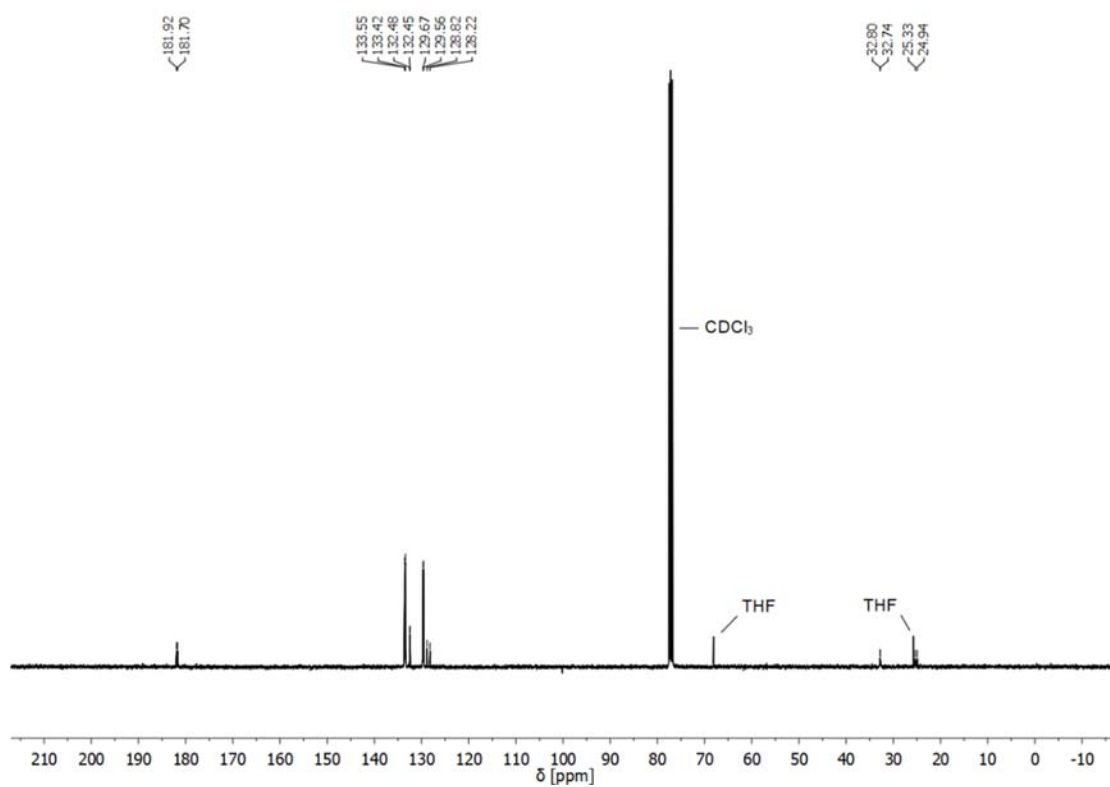


Figure S30. $^{13}\text{C}\{^1\text{H}\}$ NMR spectrum of compound **6** in CDCl_3 (101 MHz; 298 K).

IR Spectra (ATR)

IR spectra were obtained on a Bruker Tensor 37 FTIR spectrometer, equipped with a room temperature DLATGS detector and a diamond ATR (attenuated total reflection) unit.

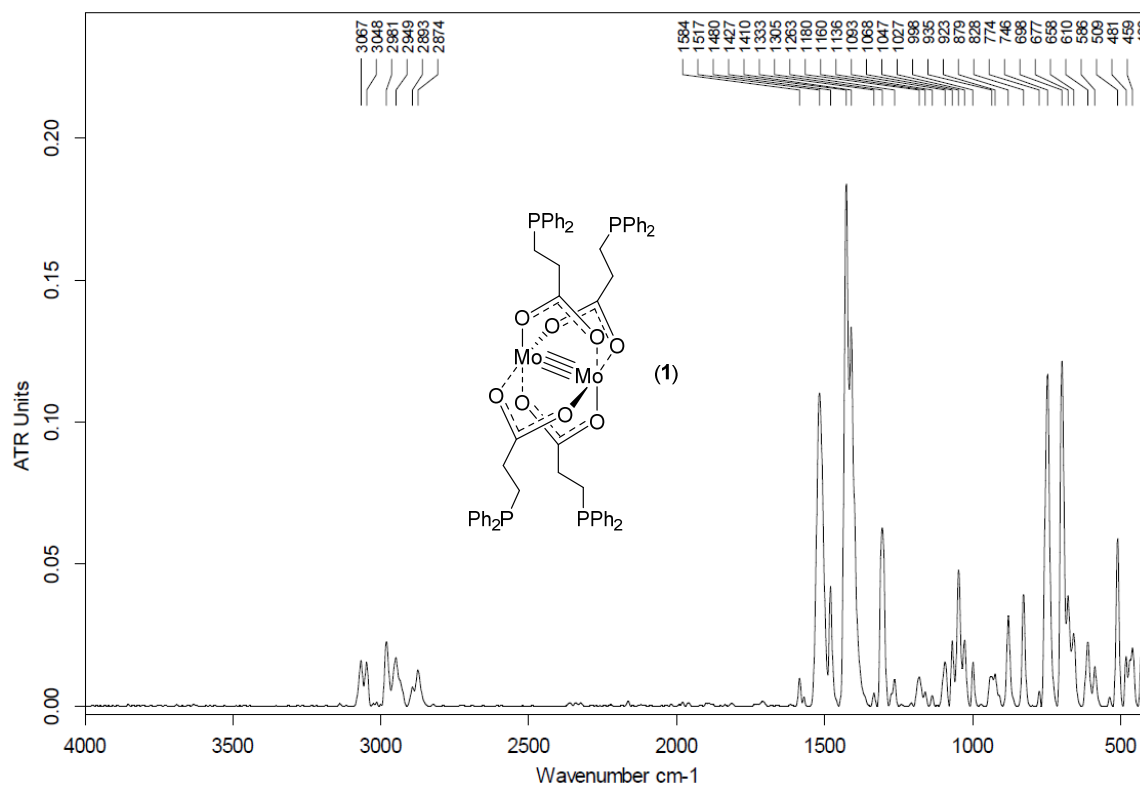


Figure S31. IR spectrum of [Mo₂(O₂C-C₂H₄-PPh₂)₄] (1).

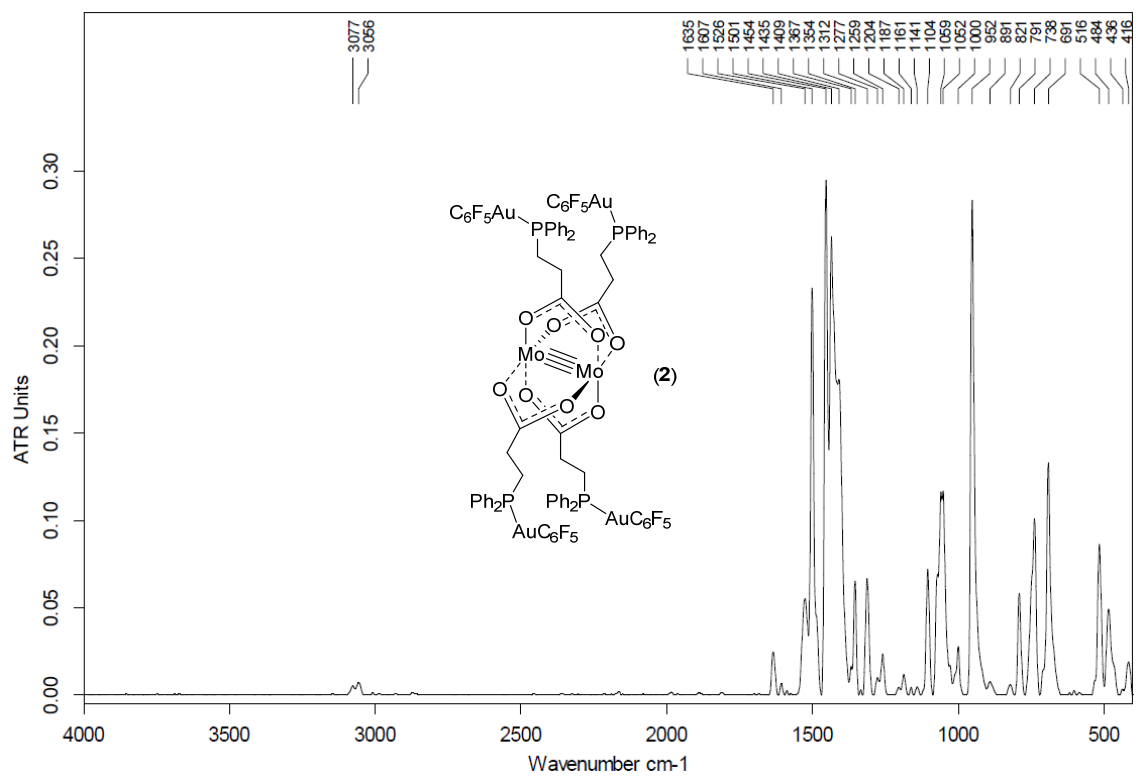


Figure S32. IR spectrum of $[\text{Mo}_2(\text{O}_2\text{C}-\text{C}_2\text{H}_4-\text{PPh}_2)_4(\text{AuC}_6\text{F}_5)_4]_2$ (2).

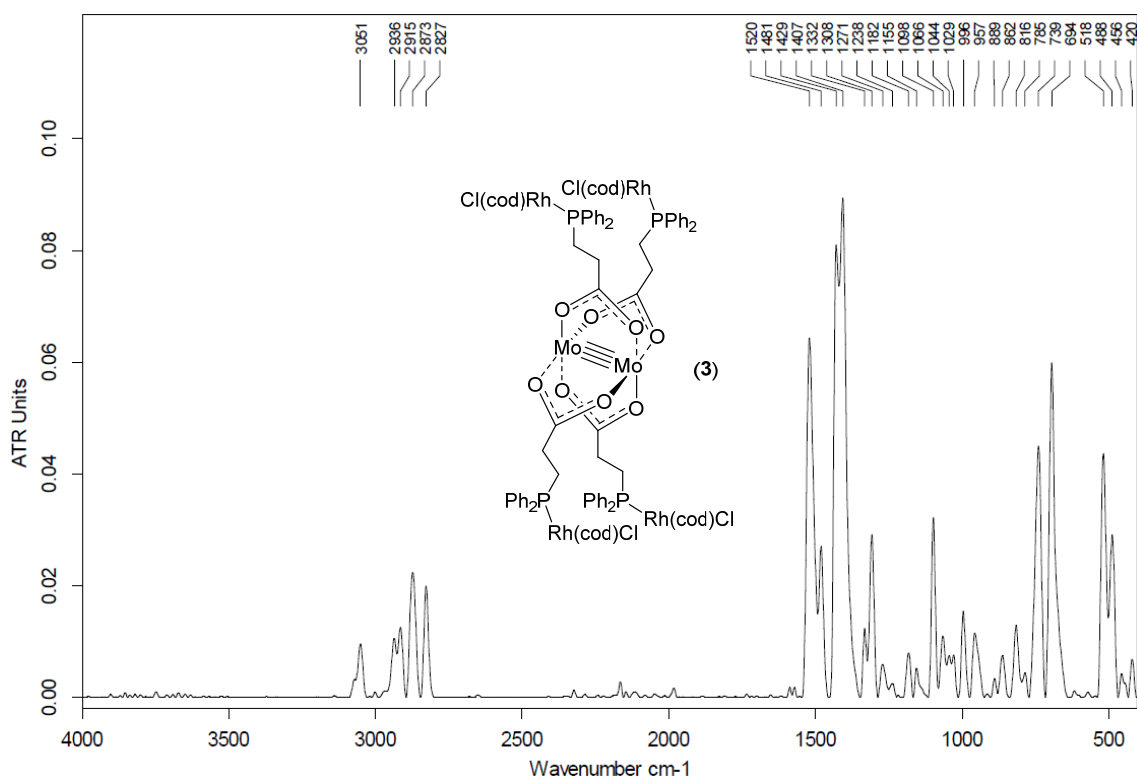


Figure S33. IR spectrum of $[\text{Mo}_2(\text{O}_2\text{C}-\text{C}_2\text{H}_4-\text{PPh}_2)_4(\text{RhCl}(\text{cod}))_4]$ (3).

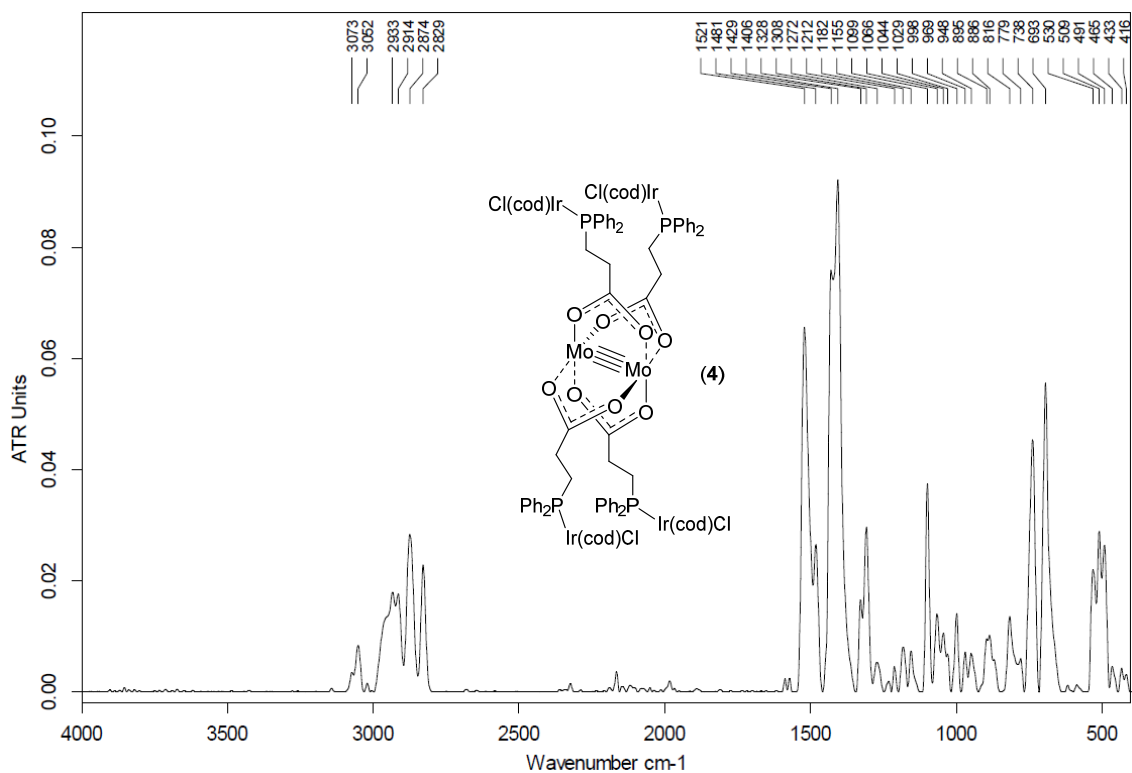


Figure S34. IR spectrum of $[\text{Mo}_2(\text{O}_2\text{C}-\text{C}_2\text{H}_4-\text{PPh}_2)_4(\text{IrCl}(\text{cod}))_4]$ (**4**).

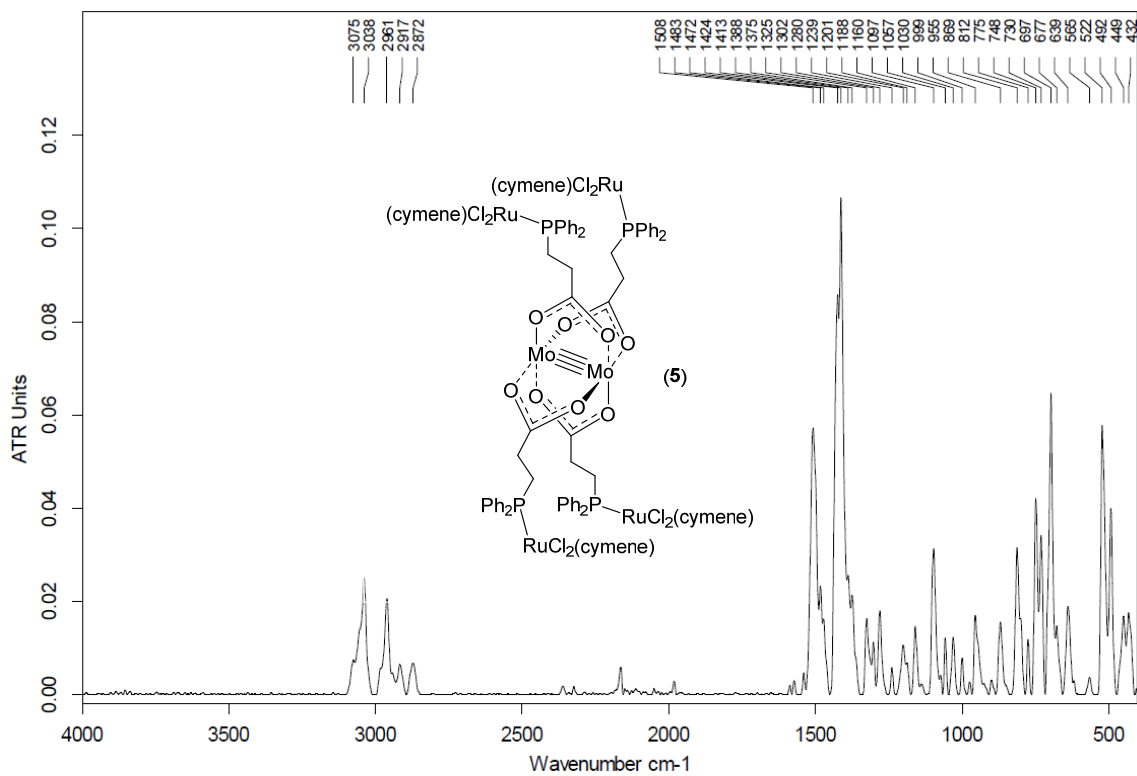


Figure S35. IR spectrum of $[\text{Mo}_2(\text{O}_2\text{C}-\text{C}_2\text{H}_4-\text{PPh}_2)_4(\text{RuCl}_2(\textit{p}\text{-cymene}))_4]$ (**5**).

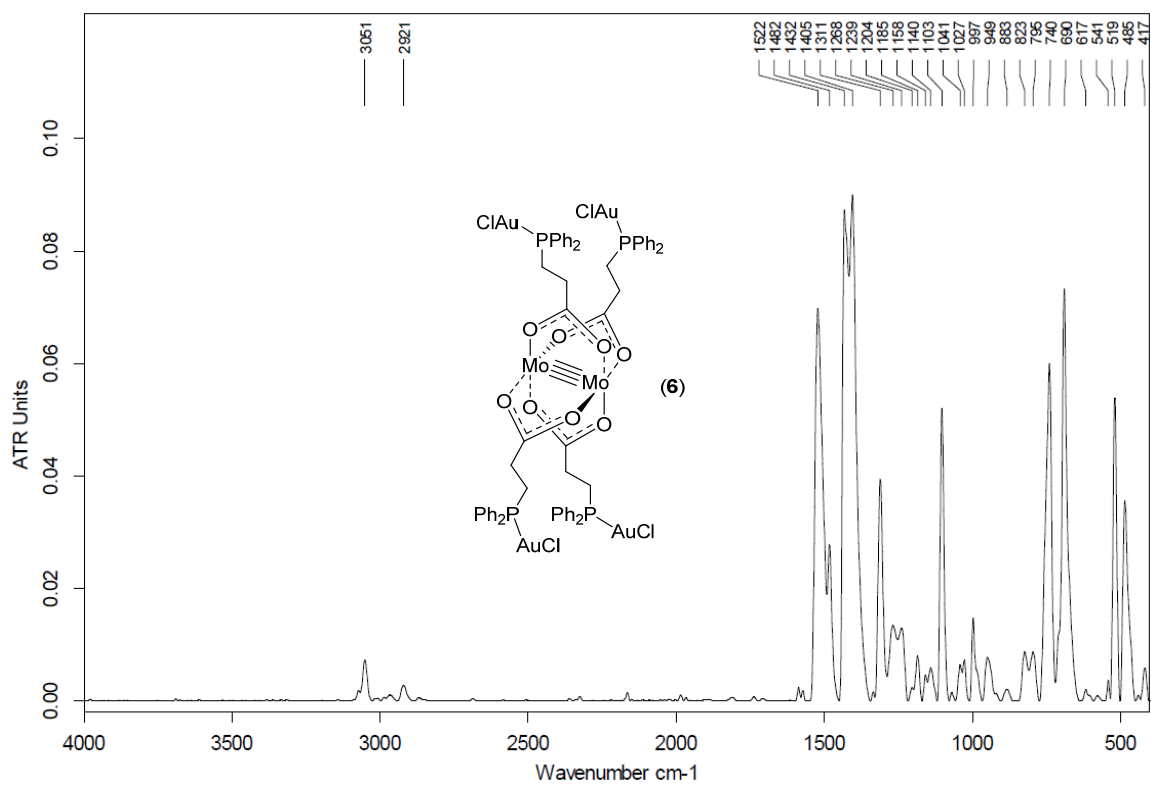


Figure S36. IR spectrum of $[\text{Mo}_2(\text{O}_2\text{C}-\text{C}_2\text{H}_4-\text{PPh}_2)_4(\text{AuCl})_4]$ (**6**).

Photoluminescence Spectra

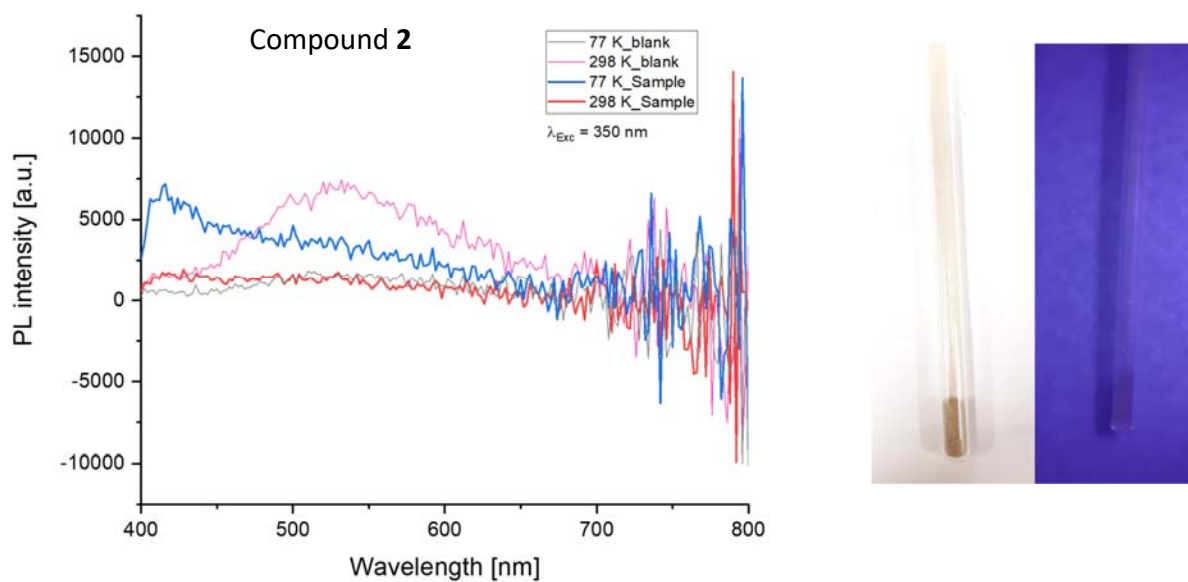


Figure S37. Photoluminescence spectrum of compound **2** after excitation at 350 nm and detection between 400 and 800 nm (at $T = 77$ K and 298 K). No relevant emission bands are detected.

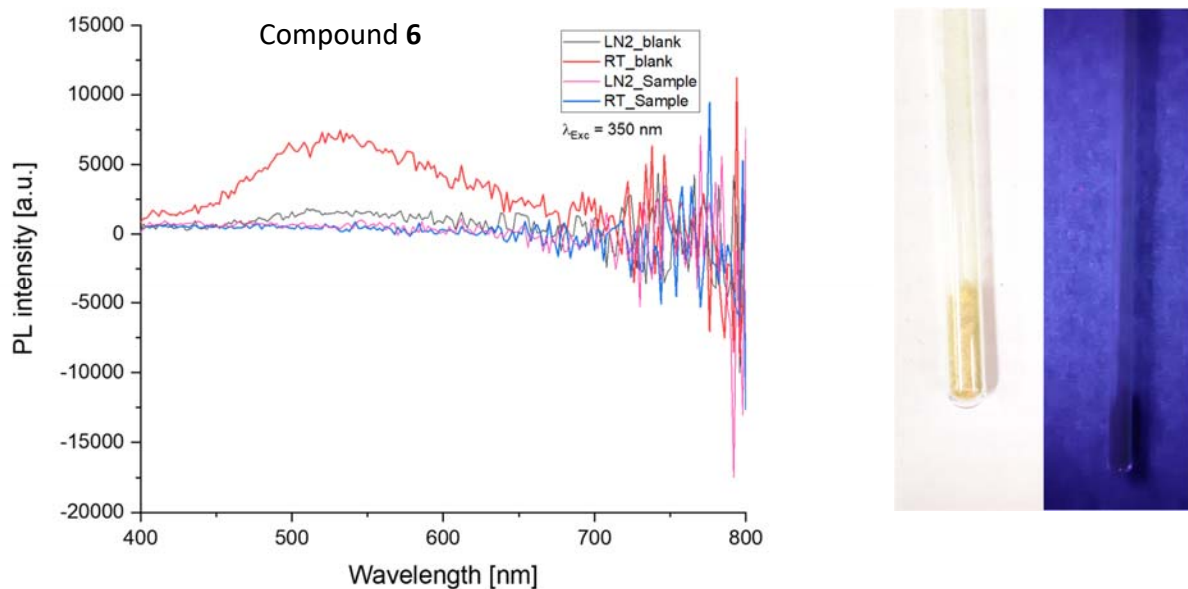


Figure S38. Photoluminescence spectrum of compound **6** after excitation at 350 nm and detection between 400 and 800 nm (at $T = 77$ K and 298 K). No relevant emission bands are detected.

Bibliography

1. G. Sheldrick, *Acta Crystallogr. Sect. A*, 2008, **64**, 112-122.
2. G. Sheldrick, *Acta Crystallogr. Sect. C*, 2015, **71**, 3-8.
3. O. V. Dolomanov, L. J. Bourhis, R. J. Gildea, J. A. K. Howard and H. Puschmann, *J. Appl. Crystallogr.*, 2009, **42**, 339-341.